REPORT DOCUMENTATION PAGE

Form Approved
OMB No. 0704-0188

1. AGENCY USE ONLY (Leave blank)	2. REPORT DATE	3. REPORT TYPE AND DATES COVERED
	5/26/94	Final Progress Report

4. TITLE AND SUBTITLE

High Power, High Frequency Radiation from Beam-Plasma Interactions

5. FUNDING NUMBERS

61102F
2301/ES

6. AUTHOR(S)

Dr. Gregory Benford

7. PERFORMING ORGANIZATION NAME(S) AND ADDRESS(ES)

University of California, Irvine
Department of Physics
Irvine, CA 92717

8. PERFORMING ORGANIZATION REPORT NUMBER

AFOSR-90-0255

AFOSR-TR- 95 0117

9. SPONSORING/MONITORING AGENCY NAME(S) AND ADDRESS(ES)

AFOSR/NE
110 Duncan Avenue
Bldg. 410, Suite B115
Bolling AFB, DC 20332-0001

10. SPONSORING/MONITORING AGENCY REPORT NUMBER

AFOSR-90-0255

11. SUPPLEMENTARY NOTES

12a. DISTRIBUTION/AVAILABILITY STATEMENT

APPROVED FOR PUBLIC RELEASE: DISTRIBUTION UNLIMITED

12b. DISTRIBUTION CODE

13. ABSTRACT *(Maximum 200 words)*

The attached papers sum up our program's research for the last inclusive funding period. This is the final report.

14. SUBJECT TERMS			15. NUMBER OF PAGES
			16. PRICE CODE
17. SECURITY CLASSIFICATION OF REPORT	18. SECURITY CLASSIFICATION OF THIS PAGE	19. SECURITY CLASSIFICATION OF ABSTRACT	20. LIMITATION OF ABSTRACT

Air Force Office of Scientific Research

AFOSR-90-0255

Final Progress Report

High Power, High Frequency Radiation from Beam-Plasma Interactions

Our work is reflected in the attached papers.

Electric Field Measurement in a Plasma-Filled X-Band BWO, Zhai, X., Garate, E., Prohaska, R., and Benford, G., Phys. Lett. A **186** 330-334 (1994).

Plasma Density Measurement in a Gas-Filled X-band Backward Wave Oscillator with a Double Conversion Heterodyne Microwave Interferometer, Zhai, X., Garate, E., Prohaska, R., and Benford, G., (1992).

Experimental Study of a Plasma-Filled Backward Wave Oscillator, Zhai, X., Garate, E., Prohaska, R., Benford, G., and Fisher, A., to be published in IEEE Plasma Science, February 1993.

21 March 1994

PHYSICS LETTERS A

ELSEVIER

Physics Letters A 186 (1994) 330–334

Electric field measurement in a plasma-filled X-band backward wave oscillator

Xiaoling Zhai, Eusebio Garate, Robert Prohaska, Amnon Fisher, Gregory Benford

Department of Physics, University of California, Irvine, CA 72717, USA

Received 12 February 1993; revised manuscript received 23 November 1993; accepted for publication 10 January 1994
Communicated by M. Porkolab

Abstract

The electric field in a plasma-filled X-band backward wave oscillator (BWO) was measured by the Stark-effect method. Field strengths were as high as 110 kV/cm when the BWO power level was ~75 MW. Observed electric fields lasted throughout the ~60 ns high power microwave pulse. After this pulse, fields 30 to 40 kV/cm persisted until beam shutoff, presumably arising from beam–plasma turbulence and low power level electromagnetic radiation.

Low power backward wave oscillators (BWOs) are well developed and understood microwave devices. However, high power vacuum BWOs driven by intense, relativistic electron beams (REB) still raise basic physics questions. Recently, addition of plasma in BWOs has become a research topic of interest. Since the first plasma-filled slow wave device [1] reported in 1975, researchers have found that plasma-filled BWOs have many desirable properties, among them higher microwave power output, higher efficiency [2] and frequency tunability for different plasma density [3]. In addition to these features, plasma provides a medium for us to diagnose the interaction between the REB, slow wave structure and the electromagnetic waves. The goal of this experiment was to measure the electric field strength in a plasma-filled BWO, using the changes in the relative amplitude of helium emission lines due to the high power microwave electric fields (AC Stark shift).

Spectroscopic methods can be employed in high level electromagnetic noise (ranging from microwave to X-ray), low repetition rate experiments (such as the generation of high power microwaves with REB experiments). They can measure properties of the fields without interfering with the system. Such time resolved methods have been used in many laboratories [4–7] since Baranger and Mozer suggested using the high-frequency Stark effect as a diagnostic tool to study the frequency and strength of the electrostatic fluctuations in a plasma [8]. We used helium plasma for this experiment, choosing the four energy-level system (3^1P, 3^1D, 2^1P, 2^1S) of helium I for the spectroscopic measurement. Transitions from 3^1P to 2^1S ($\lambda_A = 501.56$ nm) and from 3^1D to 2^1P ($\lambda = 667.80$ nm) are allowed, and the transition from 3^1P to 2^1P is forbidden ($\lambda_F = 663.20$ nm) in the electric dipole approximation. In a perturbing electric field, energy levels 3^1D and 3^1P are mixed. Under this circumstance it is possible to see photons from the forbidden line. The perturbing electric field strength can be calculated by the forbidden ($\lambda_F = 663.20$ nm) and allowed ($\lambda_A = 501.56$ nm) line intensity ratio I_F/I_A [6],

$$E = 305.8 (I_F/I_A)^{0.5} \text{ kV/cm} . \quad (1)$$

Fig. 1 is the experimental setup. A 650 kV, 1.6 kA,

SSDI 0375-9601(94)00054-S

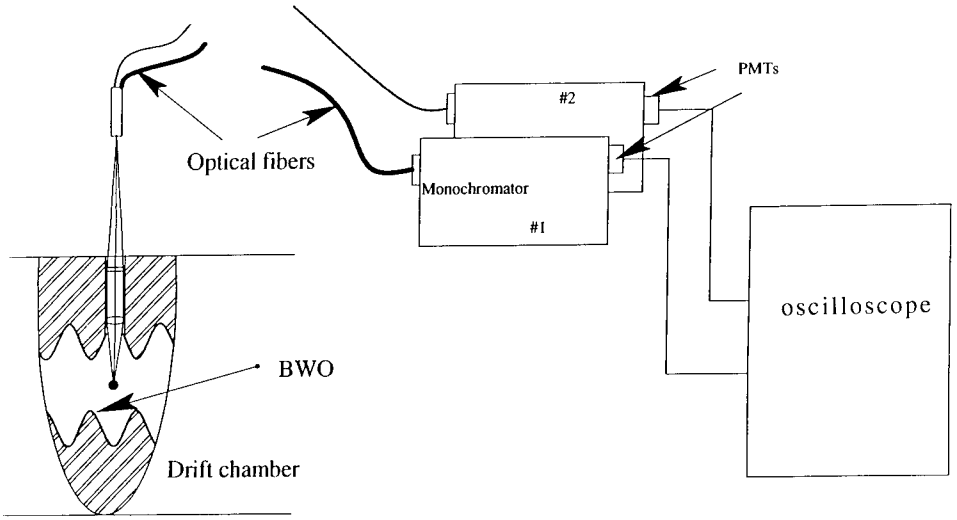

Fig. 1. Experimental setup.

500 ns annular electron beam with $R=9$ mm and $\Delta R=2$ mm enters the BWO along the 15 kG guiding magnetic field. The BWO is a cylindrical waveguide with a periodically varying wall radius, $R(z)$, sinusoidally rippled about the mean radius, R_0, such that

$$R(z)=R_0+h\cos(k_0 z)\,,\quad k_0=2\pi/z_0\,, \tag{2}$$

where $h=0.45$ cm is the ripple amplitude, $z_0=1.67$ cm is the period and $R_0=1.45$ cm. Our window for the spectroscopic measurement was on the 9th ripple of the BWO (total of 10 ripples). Plasma was generated by electron beam impact ionization of the background neutral helium. An X-band horn placed 2 m from the end of the drift chamber received the X-band microwaves from the BWO.

Light emission from the BWO was collected with lenses and focused onto a pair of optical fibers, one for the forbidden line and one for the allowed line. The two fibers were placed close together at the focal point of the collecting lenses, then routed to the monochromators located in a screen room about 20 m away. The collection lenses consisted of a doublet; the first lens had the lowest possible f-number for high light gathering efficiency, the f-number of the second lens was chosen to match the fibers. Both fibers were quartz, which has high efficiency and does not produce much light when hit by background X-rays. A 1 mm core diameter fiber looked at the allowed $\lambda=501.56$ nm line from the helium. We used a bundle made of 50 small fibers to improve light gathering efficiency of the forbidden line. Each fiber had a 200 μm diameter. The end near the light source was circular with 1.6 mm diameter, the other end was a 12 mm long flat array to match the entrance slit of the monochromator. Each monochromator had a holographic blazed grating with 1800 grooves/mm; the reciprocal linear dispersion of the instruments was 0.7 nm/mm. The detectors were Hamamatsu R 1894 and R 1635 photomultiplier tubes, both with 0.8 ns rise time. Outputs from the photomultiplier tubes were then recorded by a fast oscilloscope. The temporal resolution of this spectral system is determined by the photomultiplier tubes, it is <1.6 ns. To prevent systematic error, the spectroscopic system was calibrated daily with a helium discharge lamp. Since the helium lamp does not produce the $\lambda=663.2$ nm forbidden line, we had to choose the $\lambda=667.8$ nm line and the $\lambda=501.56$ nm line to calibrate our system. The error introduced by using $\lambda=667.8$ nm to calibrate the forbidden line collection optics efficiency at $\lambda=663.2$ nm is negligible since the photon cathode sensitivity of the photomultiplier and the transmission rate of the optical fiber changes very little under wavelength changes from $\lambda=663.2$ to 667.8 nm. We measured the ratio of line intensities ($\lambda=667.8$ to $\lambda=501.56$ nm) of our helium lamp with a photomultiplier tube and a monochromator since a standard light source was not available to us. The frequency

response of the photomultiplier tube and the monochromator were provided by the manufacturers (monochromator efficiency ratio $e(\lambda=667.8\ \text{nm})/e(\lambda=501.56\ \text{nm})=79.4\%$; photomultiplier tube efficiency ratio $e(\lambda=667.8\ \text{nm})/e(\lambda=501.56\ \text{nm})=33.7\%$). Our direct measurement gave the intensity ratio of these two lines $\alpha_m=I_m(\lambda=667.8\ \text{nm})/I_m(\lambda=501.56\ \text{nm})=2.12$. Then the line intensity ratio of our helium lamp should be $\alpha=I(\lambda=667.8\ \text{nm})/I(\lambda=501.56\ \text{nm})=2.12/33.7\%\times 79.4=7.9$. This line intensity ratio was used in Eq. (1) when we calculated the electric field with the measured forbidden and allowed line intensity ratio $(I_F/I_A)_{\text{measur}}$.

The main error of this experiment is due to the collected photon number changes from shot to shot. In order to be sure that only the helium emission could be recorded by the photomultiplier. With no helium in the system, we only observed a total of 2–3 photons from each monochromator in more than 20 shots we fired. With helium in the system, we normally got 7–10 photons in the forbidden line and more than 20 photons (after a 1.5 neutral density filter) in the allowed line. This indicated the background noise was negligible. The main error in this measurement was due to the fluctuation of the photon number from shot to shot.

Fig. 2 shows the oscilloscope traces of the forbidden line, allowed line photons and the BWO microwave emission. Forbidden line photons appear with the high power microwave emission, while allowed line photons appear earlier and last much longer than the microwave pulse. This is because the forbidden transition only happens when there is electric field in the system, while the allowed transition occurs as long as there is plasma in the system. This suggests that the electric field which induces the forbidden transition was produced by the high power microwaves. We counted photon numbers in each time interval for both the forbidden and allowed lines in each shot, then averaged over ~100 shots. The ratio of the average photon numbers in the forbidden and allowed lines was used to calculate the electric field using Eq. (1).

Fig. 3 shows the results of electric field measurement in the plasma-filled BWO when the microwave was enhanced by the background plasma by a factor of 2 over its vacuum counterpart [3] (this enhancement could be as high as a factor of 7 with a 3 kA beam current, but then the microwave pulse duration will drop to ~20 ns). The measured microwave power was 75 ± 10 MW and the microwave pulse duration (FWHM) was ~60 ns. Fig. 3 shows the

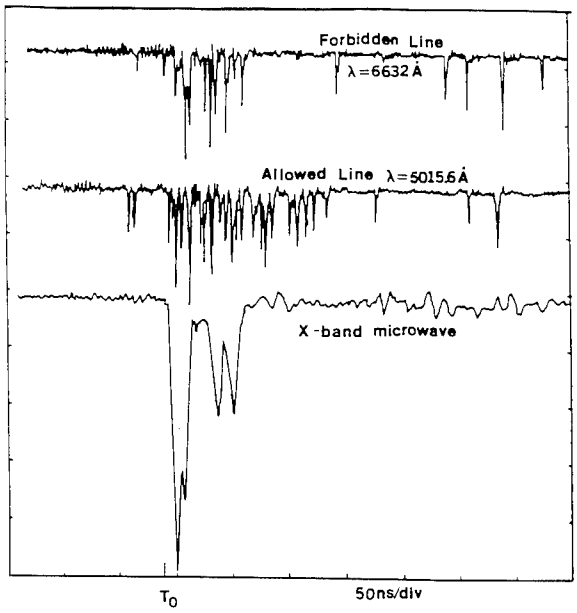

Fig. 2. The oscilloscope traces of the forbidden line, allowed line photons and the BWO microwave emission. Here $T_0=140$ ns is counted from beam voltage turn on.

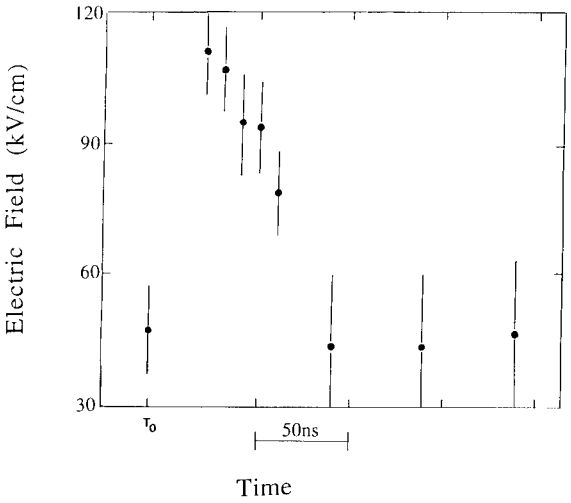

Fig. 3. Electric field versus time when the BWO microwave power was enhanced by the background plasma. Statistical error due to the photon number fluctuation was 30% during the peak microwave electric field and 60% off the peak region. $T_0=140$ ns is counted from beam voltage turn on.

strongest electric fields also lasted ~60 ns, with maximum ~110 kV/cm. Then $\sqrt{\langle E^2 \rangle}$ dropped to ~40 kV/cm.

Clearly this electric field peak correlates with the observed microwaves, since they turned on and off at the same time. After the microwave pulse, the measured electric field did not drop to zero but stayed at ~40 kV/cm. The noise level in this time period is very high, so $\sqrt{\langle E^2 \rangle}$ is more uncertain. Statistical error due to photon number fluctuation was 30% during the peak microwave electric field. The error was more than 60% off the peak region, due to the small number of photons received each shot.

When the background helium pressure increased above 150 mTorr, the X-band microwaves turned off. At the same time a microwave signal appeared in the Ku-band with a center frequency of 14.6 GHz and ~150 ns pulse duration. This is the mode switching from the TM_{01} mode to the TM_{02} mode in the plasma-filled BWO, as previously reported [9].

The measured electric field strength after mode switching was about 56 kV/cm (Fig. 4) and lasted 150 ns, as long as the TM_{02} microwave pulse. Again we can see that after the microwaves turned off, the background field did not cease but dropped to ~30 kV/cm. The electric field produced by the background plasma is ~30 kV/cm (see Fig. 4).

From both Figs. 3 and 4, we can see the electric field did not drop to zero after the microwaves turned off, but stayed at the level 30–40 kV/cm. Presumably this is the field arising from a combination of beam–plasma turbulence and other waves such as Trivelpiece–Gould modes [12], low power level radiation of TM_{01}, etc. (Because of the high attenuation we put in front of the crystal diode, radiation at power levels lower than 100 kW would not be detected.) Thus these electric fields are at least ~30 kV/cm. The electric field of the high power microwaves

$$\sqrt{\langle E_M^2 \rangle} = \sqrt{\langle E_{\text{total}}^2 \rangle - (\Delta E)^2} \approx 100 \text{ kV/cm} .$$

Here $\Delta E \approx 30$–40 kV/cm. We neglected the cross term [11], which should be small.

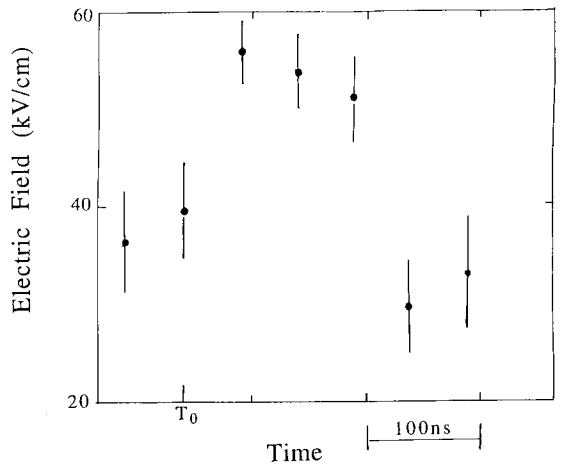

Fig. 4. Electric field versus time when mode switching occurred. Statistical error due to the photon number fluctuation was 30% during the peak microwave electric field and 60% off the peak region. $T_0 = 140$ ns is counted from beam voltage turn on.

To estimate how much microwave power this field strength implies, assume a smooth wall tube with radius $R = 1.9$ cm (since this electric field measurement was done at the wide part of the BWO with $R = 1.9$ cm). Assuming a TM_{01} mode propagating along the axis of this drift tube, which was filled with uniform plasma $n_p = 8 \times 10^{11}$ cm^{-3}, we have [10]

$$S = \frac{c}{8\pi} \sqrt{\epsilon/\mu}\, (\omega/\omega_\lambda)^2 \sqrt{(1-\omega^2/\omega_\lambda^2)} E_0^2 \times \int_0^{R_0} [J_n(x_n r/R_0)]^2 2\pi r \, dr . \quad (3)$$

Here S is the microwave power flux in the tube of frequency ω and ω_λ is the cutoff frequency, x_n is the first root of J_n, and E_0 is the amplitude of the electric field. For the TM_{01} mode $\omega/2\pi = 9.5$ GHz, the center microwave frequency of the plasma-filled BWO. The cutoff frequency $\omega_{\lambda/2\pi} = 6.0$ GHz and $J_n = J_0$. We measured $\sqrt{\langle E_M^2 \rangle} \approx 100$ kV/cm. To get E_0^2 we have

$$\sqrt{\langle E^2 \rangle} = E_0^2 \frac{\int_{-R}^{R} (E_r^2 + E_Z^2)\, dr}{2R} \approx 0.5 E_0^2 . \quad (4)$$

Eqs. (2)–(4) give $S \approx 110 \pm 60$ MW, with the uncertainty due to the 30% error in the electric field measurement. Direct microwave power measurement gives 75 ± 10 MW. Using the same method, we calculated $S = 4$ MW for the TM_{02} mode.

The measured electric field also includes fields produced by the electron beam charge, and fields of other waves (Trivelpiece–Gould modes [12]) in the plasma-filled BWO. Electric fields from the electron beam charge are not important here. We used a 1 kA

beam and more than 120 mT of background helium gas in the BWO. The measured plasma density was as high as 8×10^{11} cm^{-3} where the microwave pulse appeared and the electric field peaked, while the beam density was only $\sim10^{11}$ cm^{-3}. Therefore, the beam was charge neutralized. (The Trivelpiece–Gould mode had 20 dB less power than the X-band TM_{01}. It only produces ~1 kV/cm, so can be ignored here.)

To accurately calculate the power flux in the BWO, one has to assume the electric field distribution in the BWO in such a form as in Ref. [13], including the sinusoidal structure. One also must calculate the light collecting efficiency of the optical system as a function of position in the BWO. Then one must find the average electric field and use the measured electric field value to calculate the power flux in the BWO. This very complex calculation demands a numerical solution, which lies beyond our present program. Our sample estimation here agrees with experimental results in the error range.

In conclusion, we measured the average electric field strength in a plasma-filled backward wave oscillator as it varied in time, while the microwave power output was enhanced by the background plasma. The electric field peaked at 110 kV/cm and lasted only as long as the high power microwave pulse (~75 MW). We also measured the electric field (peak ~56 kV/cm) as a function of time while the BWO plasma density $>10^{12}$ cm^{-3} and when the "mode switch" occurred. These *E*-field levels can significantly affect beam quality and scattering, and may be implicated in the shut off of microwaves, in ~60 ns.

We thank Dr. K. Kato, David Sar and General Dynamics, Pomona Division, for the use of their equipment. This work was supported by AFOSR under contract no. 90-0255.

References

[1] Yu.V. Tkach et al., Fiz. Plazmy 1 (1975) 81 [Sov. J. Plasma Phys. 1 (1975) 43].
[2] K. Minami, W.R. Lou, W.W. Destler, R.A. Aehs, V.L. Granatstein and Y. Carmel, Appl. Phys. Lett. 53 (1988) 559.
[3] X. Zhai, E. Garate, R. Prohaska and G. Benford, Appl. Phys. Lett. 60 (1992) 2332.
[4] H.-J. Kunze and H.R. Griem, Phys. Rev. Lett. 21 (1968) 1048.
[5] A. Dovrat and G. Benford, Phys. Fluids B 1 (1989) 2488.
[6] K. Kawasaki, T. Usui and T. Oda, J. Phys. Soc. Japan 51 (1982) 3666.
[7] G.C.A.M. Janssen, E.H.A. Granneman and H.J. Hopman, Phys. Fluids 27 (1984) 736.
[8] M. Baranger and B. Mozer, Phys. Rev. 123 (1961) 25.
[9] Y. Carmel, K. Minami, W.R. Lou, R.A. Kehs, W.W. Destler, V.L. Granatein, D.K. Abe and J. Rodgers, IEEE Trans. Plasma Sci. 18 (1990) 497.
[10] J.D. Jackson, Classical electrodynamics, 2nd Ed. (Wiley, New York) p. 347.
[11] H.R. Griem, Spectral line broadening by plasmas (Academic Press, New York, 1974) p. 153.
[12] X. Zhai, E. Garate, R. Prohaska and G. Benford, Phys. Rev. A 45 (1992) 8336.
[13] K. Minami, Y. Carmel, V.L. Granatein, W.W. Destler, W.R. Lou, D.K. Abe, R.A. Kehs, M.M. Ali, T. Hosokawa, K. Ogura and T. Watanabe, IEEE Trans. Plasma Sci. 18 (1990) 537.

Plasma Density Measurement in a Gas-Filled X-band Backward Wave Oscillator With a Double Conversion Heterodyne Microwave Interferometer

Xiaoling Zhai, Eusebio Garate, Robert Prohaska, and Gregory Benford

Physics Department, University of California, Irvine, CA 92717

Abstract

Plasma density was measured with a heterodyne microwave interferometer in both a gas-filled X-band backward wave oscillator (BWO) and in a smooth tube. Plasma is generated by impact ionization of a 700 kV, 2 kA electron beam. For fixed gas pressure we found that the plasma density in the BWO was much higher than in a smooth tube, indicating that high power microwaves were important in forming plasma in the neutral-gas filled BWO. While the BWO microwave output power was enhanced by the additional plasma in the BWO (110 mT), the measured plasma density was $n_{cr} \sim 3 \times 10^{12}$ cm^{-3} at the turn on of the emitted microwave pulse.

PACS numbers: 52.40.Fd, 52.75.Ms, 52.23. Sw

Backward wave oscillators (BWO) excited by intense relativistic electron beams (REB) are very promising high power microwave sources. This type of device has been studied in many laboratories[1-5] since Nation[6] first confirmed the possibility in 1970. Injecting plasma into the slow wave structure[7,8] enhances power emission by factors of 3 to 8. A plasma-filled BWO can convert beam kinetic energy into microwave radiation with efficiency as high as 40%, a significant improvement over the 5 % typical for vacuum[8]. However, the basic mechanisms of the system are still not well understood, such as how the plasma enhances the BWO efficiency.

Measuring plasma density is crucial to quantitatively understanding plasma-filled BWOs. This can be done in several ways, e. g., using Langmuir probes and microwave interferometers. Langmuir probes are very effective for "quiet" plasma density and temperature measurements. However, a BWO normally operates with multiple kilo ampere, MV energy electron beams, so probes do not survive many shots. Strong magnetic fields further complicate the interpretation of data. Since microwave interferometers are non-perturbing and offer good time resolution, we used them to measure the plasma density, $n_p(t)$. Our experiment used a 35 GHz 2 stage heterodyne interferometer, motivated principally by the fact that the beam radiated appreciable power in the band used for the measurements. A waveguide-type bandpass filter (30 - 35 GHz) proved unable to cut off the beam noise. Using heterodyne techniques coupled with narrow bandpass filters, we managed to exclude beam noise in our measurement. A second conversion was added simply to make the output visible on a conventional oscilloscope. In addition, the heterodyne technique transfers the problem of detecting a small phase shift at 35 GHz to phase shifts at ~ 50 MHz. This makes the measurement much easier and increases sensitivity. We used 35 GHz was used as the probe frequency since this permits plasma density measurement up to 1.5×10^{13} cm^{-3}.

In our experiment (Fig. 1), a Marx capacitor bank generates a 650 kV, 2 kA electron beam with 500 ns pulse duration. The beam is annular with 1.8 cm diameter and 2 mm thickness, and is injected into the BWO along a 15 kG guiding magnetic field. The BWO is a cylindrical waveguide with a periodically varying wall radius, R(z), sinusoidally rippled about the mean radius, R_0, such that

$$R(z)=R_0+h\cos(k_0 z) \qquad k_0=2\pi/z_0$$

where h=0.45 cm is the ripple amplitude, z_0=1.67 cm is the period and R_0=1.45 cm. (This BWO is a copy of that in Ref. 8) with two observation windows at the 9-th ripple. We used these to mount waveguide into and out of the slow wave structure. An X-band horn 2 meters from the end of the drift tube received the TM_{01} radiation from the BWO.

Plasma was generated by background helium ionization from the electron beam. The plasma density measurement was done in two steps. At first, we replaced the BWO with a 19 mm diameter smooth tube and kept the same A-K gap. This way we could see the effect of the strong microwave radiation from the BWO in plasma production by comparing with plasma density in a BWO. For this part of the experiment we used a 10 kW, 4 μs pulse duration, 9.6 GHz X-band magnetron as the microwave source for the interferometer. The magnetron microwave went through the plasma, carrying information about $n_p(t)$ in its phase change $\Delta\phi(t)$. The probe microwave then mixed with microwave from a local oscillator, yielding a mixed frequency of 30 ~100 MHz. $\Delta\phi(t)$ occurs in the frequency difference $f_M(t)=f_{magnetron}-f_{oscillator}$ as a frequency change $\Delta f_M(t)$. We get $\Delta\phi(t)$ by comparing this new frequency to the unshifted mixed frequency $f_{M0}=f_M(t<t_0$,with t_0 the beam start time), so that $\Delta f_M(t)=f_M(t)-f_{M0}$. With no plasma in the system we detected no shift in the frequency difference Δf_{M0}, for up to 3 μs. We synchronized the beam voltage pulse with the stable portion of the mixed frequency. This method will cause an underestimate of the real plasma density in the plasma-filled BWO because of the absence of the high power microwave which may

provide additional ionization of the background neutral gas. Fig. 2 shows the density measurement for different background neutral gas pressures in a smooth wall tube. T=0 ns is the start time of our beam pulse. At T=140 ns, n_p was about $8x10^{11}$ cm^{-3} for P_{He}=120 mTorr.

Fig. 3 shows the experimental setup for measuring the plasma density in a gas-filled BWO. Based on the previous gas-filled smooth tube plasma density measurement, we used a Ka-band 34.5 GHz, 100 kW magnetron as a microwave source. This 34.5 GHz interferometer overcame the limitation of the X-band interferometer ($n_p<10^{12}$ cm^{-3}) could measure plasma density in a higher plasma density range (10^{12} $cm^{-3}<n_p<10^{13}$ cm^{-3}). The magnetron output was split into two branches - measurement and reference arms. One beam was attenuated to ~ 1 kW then went through the BWO (the measurement arm). Then the magnetron microwave went through the BWO was guided by a 20 meter long wave guide into a screen room. Where the magnetron microwave was attenuated again and guided to a bandpass filter (30 GHz-35 GHz) which cut some of the beam noise going through the waveguide. Then we mixed with microwave from a local Ka-band sweep oscillator. The mixed microwave was detected by a Ka-band crystal detector, then fed into a narrow bandpass filter. This filter had a center frequency of 200 MHz and 20 MHz bandwidth. This filter cut off the remaining beam noise which had passed through the first conversion. Actually, a filter with 50 MHz center frequency would be more suitable for this purpose, since a 50 MHz signal is easy to observe with an oscilloscope. We didn't have one handy so we used a signal generator to convert the 200 MHz signal again to about 20 MHz to 50 MHz. Since the microwave signal was too weak from the second conversion, we used a 20 dB amplifier to increase the signal amplitude, which was detected by an crystal detector and sent to the oscilloscope. As in Fig. 2, the reference arm microwave also went through a double conversion and sent to the same oscilloscope. The plasma density in the BWO is obtained by the phase shift between the measurement arm and the reference arm microwave signals.

Addition of plasma in a BWO can enhance the BWO microwave power output[8,9]. For our BWO, with a 700 kA, 2 kA beam, the emitted microwave power output began to increase at 60 mTorr background helium pressure. Enhancement peaked at 110 mTorr, declining at higher pressure. BWO microwave pulse duration was about 20 ns to 50 ns, depending on the background gas pressure. At low background helium pressure ~10 mTorr, the BWO microwave pulse duration was ~50 ns. When the pressure increased to 110 mTorr, the emitted microwave power output was enhanced but the pulse duration dropped to 20 ~ 30 ns. The peak microwave emission power in the plasma-filled BWO was a factor 7 over its vacuum counterpart[9]. Our smooth tube measurement implies that $n_p=n_{cr}\sim 8\times10^{11}$ cm^{-3} is the critical plasma density which enhance emitted BWO microwave power, but this didn't include the effect of the high power microwaves, which can make additional plasma. Error in this measurement was about 1.5×10^{11} cm^{-3}. The X-band magnetron working frequency was 9.57 GHz, so this interferometer was not able to measure $n_p>1.1\times10^{12}$ cm^{-3}.

Fig. 4 shows the results of the density measurement for 3 different background neutral helium pressures in a BWO. Comparing with Fig. 2, we see that for the same background helium pressure, P_{He}, and the same beam current, the plasma density in the BWO was higher than for the smooth wall tube case during the BWO microwave pulse. The plasma density grows faster between 140 ns to 300 ns except for the low helium pressure P_{He}=15 mTorr case. Rapid growth of $n_p(t)$ after the BWO microwave pulse (180 - 300 ns) could be due to hot electrons, as discussed later. At 110 mTorr, $n_p=n_{cr}$ $\sim3\times10^{12}$ cm^{-3} during the microwave pulse, the true critical plasma density for microwave output enhancement. Error in this measurement was ~ 1×10^{12} cm^{-3}. For P_{He}=15 mTorr, one can see that though at ~ 300 ns, $n_p\approx n_{cr}$, but the microwave cut off long before this. During the BWO microwave pulse (140 ns to 190 ns) $n_p << n_{cr}$ and microwave power showed no plasma-aided enhancement. This implies that plasma is a necessary but not sufficient condition for radiation enhancement. Rapid high power

microwave-drive ionization may drive plasma BWO out of the optimum density region, cutting off emission.

Comparison of the plasma density in the BWO and the smooth wall tube showed that the high power microwave electric field in the BWO made a significant difference in plasma production. This is because the strong microwave fields can greatly increase the background plasma density by ionizing neutral atoms. This becomes effective if the oscillation energy of the electron, $W=(eE/\omega)^2/2m$, exceeds the ionization energy of the neutral atom, W_i. For our experiments W ~ 100 - 250 eV and for helium, W_i =24.48 eV. Generally the electron beam will have produced a density n_0 at the beginning of the microwave pulse, t_0. Plasma density n_p then follows

$$\frac{\partial n_p}{\partial t} = \frac{\partial n_d}{\partial t} + \nu_i n - \nabla^2 D n \qquad (1)$$

Here $\frac{\partial n_d}{\partial t}$ is the direct beam impact ionization, on helium at pressure P,

$$\frac{\partial n_d}{\partial t} = 1.40\text{x}10^{19}\left(\frac{I}{2kA}\right)\left(\frac{P}{0.1Torr}\right)(cm^3 s)^{-1} \qquad (2)$$

and the microwave ionization rate is

$$\nu_i = \nu_m\left(\frac{5.48\text{x}10^{-3}}{Volt}\right)\left[kT_e + W - W_i\right] \qquad (3)$$

Here the momentum collision frequency ν_m for electrons with helium neutrals is independent of energy for energies above 4 eV,

$$\nu_m = 2.37\text{x}10^{8}\left(\frac{P}{0.1Torr}\right)s^{-1} \qquad (4)$$

The diffusive term dependent on the diffusion coefficient D is generally weak for times less than a microsecond. Solution of (1) ignoring diffusion yields

$$n_p(t) = n_0 e^{\nu_i (t-t_0)} + \frac{(\partial n_d / \partial t)}{\nu_i}\left[e^{\nu_i (t-t_0)} - 1\right] \qquad (5)$$

For our experiment at 100 mTorr, the beam neutralizes its self-charge in 100 ns. After 40 ns more it produces a density $n_0(t_0) \cong 5.6\text{x}10^{11}\, cm^{-3}$, whereupon BWO microwave emission begins. This is the seed density which microwave-induced electron motion can multiply at a rate given by

$$\frac{(\partial n / \partial t)}{\nu_i} \approx \frac{1.08\text{x}10^{13}}{(T_e + W - W_i)} \qquad (6)$$

Our peak electron oscillation energy is

$$W_* = 250\, eV \left(\frac{E}{34 kV / cm} \right)^2 (\nu / 9.5 GHz)^{-2} \qquad (7)$$

The ionization frequency then is

$$\nu_i = 1.3\text{x}10^6 \left(\frac{P}{0.1 Torr} \right) \left[W + T_e - 24.48 V \right] s^{-1} \qquad (8)$$

We expect the beam electrons to substantially heat to high temperatures $T_e \sim 30$ eV, so $\nu_i \approx 3.25\text{x}10^8 (P / 0.1 Torr)\, s^{-1}$ seems plausible. This estimate depends on ν_m of equation (4), which depends on measurements at lower values of W. Trivelpiece-Gould modes in the plasma-filled BWO[10,11] can also aid ionization, with typical fields ~ kV/cm and a broad spectrum between 1 GHz and 8 GHz. For these values $W = W_{TG} \approx 2$ *to* 5, so once the beam has heated electrons to $T_e > 24.5 eV - W_{TG}$, we should see ionization by hot electrons at a rate $\sim 2.3\text{x}10^7 s^{-1}$. This will add to the direct ionization of Equation (2), which yields a typical time near the beginning of microwave emission. Thus even before microwaves begin at $t = t_0$, we should see an ionization rate roughly twice that of equation (2). Fig. 4 shows this is so: We observed a rate twice the direct collision rate. The rapid rise of $n_p(t)$ in Fig. 4 exceeds the direct rate of equation (2), but is several times smaller than predicted by equation (8). This suggests that extrapolation of the data of Refs. 12 & 13 is inadequate. Still, rapid ionization occurs, verifying our basic idea.

Including diffusion will lessen ionization rates only slightly, multiplying the right hand side of (5) by exp(-2Dt), with

$$D = (2a/d)^2 \nu_m$$

where a is the Larmor radius of the plasma electrons and d is the separation between the outer electron beam annulus and the nearest wall. We take the equivalent temperature of a plasma electron as 60 eV, since $\omega >> \nu_m$; then for a 10 kG field, $a=1.8 \times 10^{-3}$ cm. For the nearest wall dimension we take the distance to the inner edge of the BWO sinusoid, d=1 mm. This leads to a minimum diffusion time ~ 1.5 μs.

This means that even for the quite narrow operating sizes of BWOs losses across or along the field are very small during the typical 50 ns microwave pulse. During that time plasma growth should be rapid, perhaps exponential. Convective plasma loss along the magnetic field lines should take an ion thermal travel time over about 30 cm, which for even 100 eV plasma is 6 μs, long after the beam pulse ceases.

Note that we have ignored any avalanche due to inductive fields arising from changes in beam current. For the ideal current profile flat-topped in time this is true, but many of our shots have more rounded profiles. This will increase $n_p(t)$ more.

In conclusion, we measured the plasma density in both a smooth wall tube and in a BWO, with the same beam parameters and the background helium gas pressure. For the same background gas pressure, plasma density in the BWO was 6 ~ 7 times higher than in the smooth wall tube, indicating that the microwave electric fields greatly increased plasma production in the neutral-gas filled BWO. The critical plasma density which enhances BWO microwave generation is $\sim 3 \times 10^{12}$ cm $^{-3}$, more than one magnitude higher than the beam density.

We thank Dr. K. Kato, David Sar and General Dynamics, Pomona Division, for use of their equipment. This work was supported by AFOSR under contract # 90-0255.

References

1. Y. Carmel, J. Ivers, R. E. Kriel, and J. Nation, phys. Rev. Lett. 33, 1278 (1974)
2. M. Friedman, Appl. Phys. Lett 26,376 (1975).
3. V. I. Belousov, V. V. Bunkin, A. V. Gaponov-Grekhov, et al., Sov. Tech. Phys. Lett. 4, 584 (1978).
4. V. S. Ivanov, N. F. Kovalev, S. I. Krementsov, and M. D. Raizer, Sov. Tech. phys. Lett. 4,329 (1978).
5. Yu. V. Tkach, Ya. B. Fainberg, N. P.Gadetskii, et al., Ukr. Fiz. Zh. 23, 1902 (1978).
6. J. A. Nation, Appl. Phys. Lett 17, 491 (1970).
7. A. A. Kolomenskii, E. G. Krastelev, G. O. Meskhi, and B. N. yablokov. Second Symoposium on Collective Acceleration Methods, Dubna, 160, (1976) [in Russian].
8. Y. Carmel, K. Minami, R. A. Kehs, W. W. Destler, V. L. Granatstein, D. Abe, and W. L. Lou, Phys. Rev. Lett. 62,(20) 2389 (1989).
9. X. Zhai, E. Garate, R. Prohaska and G. Benford, Appl. Phys. Lett., 60,(19), May(1992).
10. X. Zhai, E. Garate, R. Prohaska, and G. Benford, Phys. Rev. A. Vol. 45, No. 12, June (1992)
11. W. R. Lou, Y. Carmel, W. W. Destler, and V. L. Granatstein, Phys. Rev. Lett. Vol. 67,No. 18, 2481 (1991).
12. S. Brown, "Introduction to Electric Breakdown in Gases", J. Wiley, New York, 1966, p 50.
13. S. Brown, "Basic Data of Plasma Physics", M. I. T. Press, Cambridge, 1959, p 137.

Figure Caption:

Fig.1 Experimental setup.

Fig.2 Plasma density vs time for the smooth wall tube for three different helium pressures. (T=0 is the beam start time).

Fig.3 Experimental setup for measuring plasma density in the BWO.

Fig.4 Plasma density vs time for the helium-filled BWO for three different helium pressures. (T=0 is the beam start time). The crosshatched area is the time period microwave appeared in the gas-filled BWO.

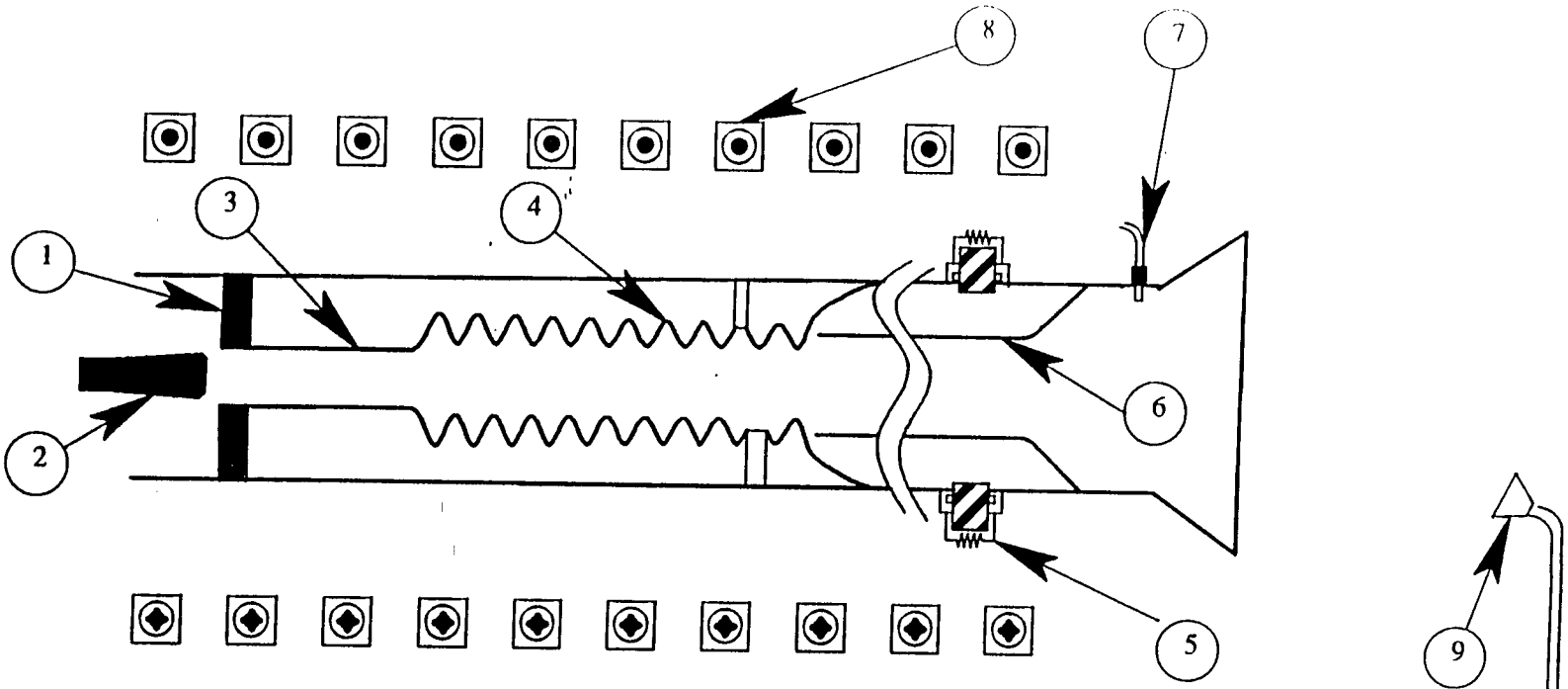

1. Anode
2. Cathode
3. Reflector
4. BWO
5. Shunt resistor
6. Beam dump
7. Helium inlet
8. Magnetic coils
9. rf receiving horn
10. Attenuator
11. 8 channel X-band rf spectrometer
12. Crystal detector
13. Oscilloscope

Fig. 1

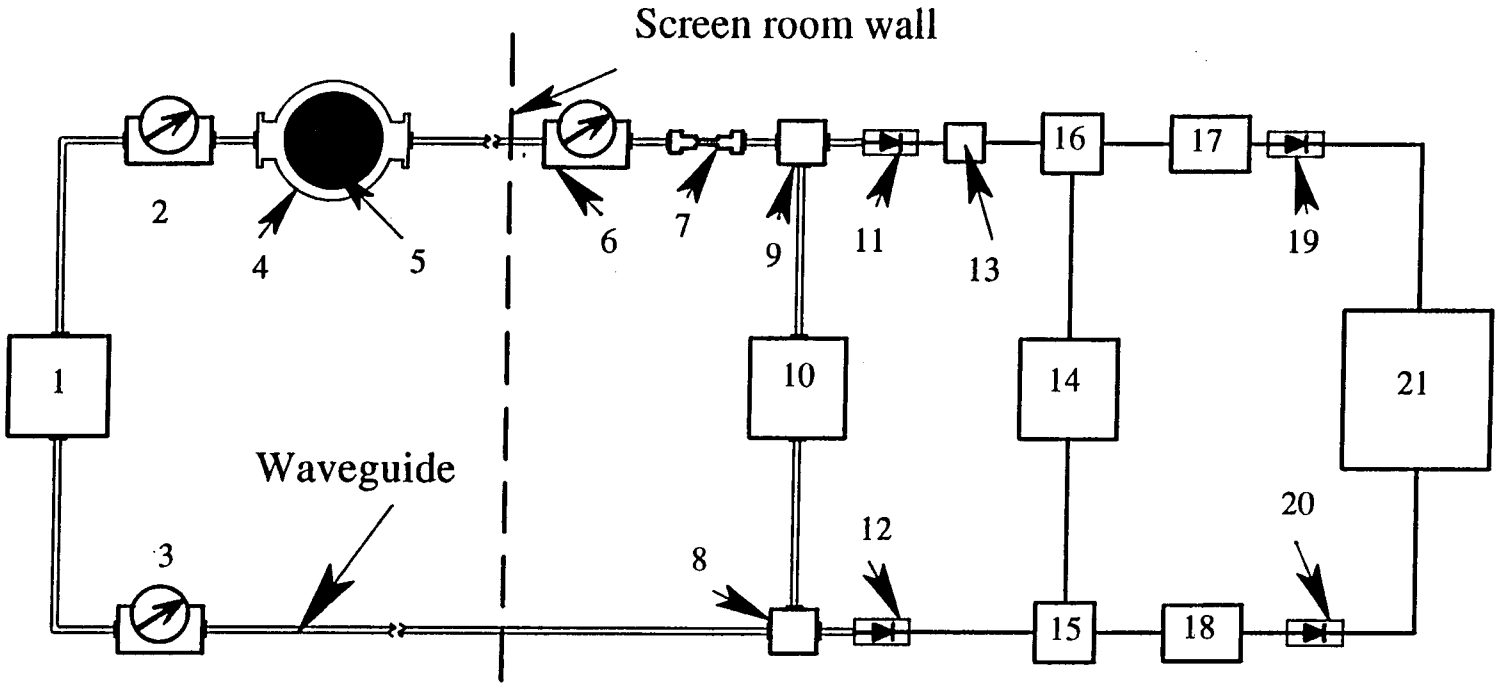

1. Magnetron
2,3,6. Varible attenuators
4. Drift chamber
5. Plasma
7. Bandpass filter
8,9. Ka-band adder
10. Ka-band sweep oscillator
11,12. Crystal detectors
13. 200MHz filter
14. Signal generator
15,16. Mixers
17,18. Amplifers
19,20. Detectors
21. Oscilloscope

Figure 2

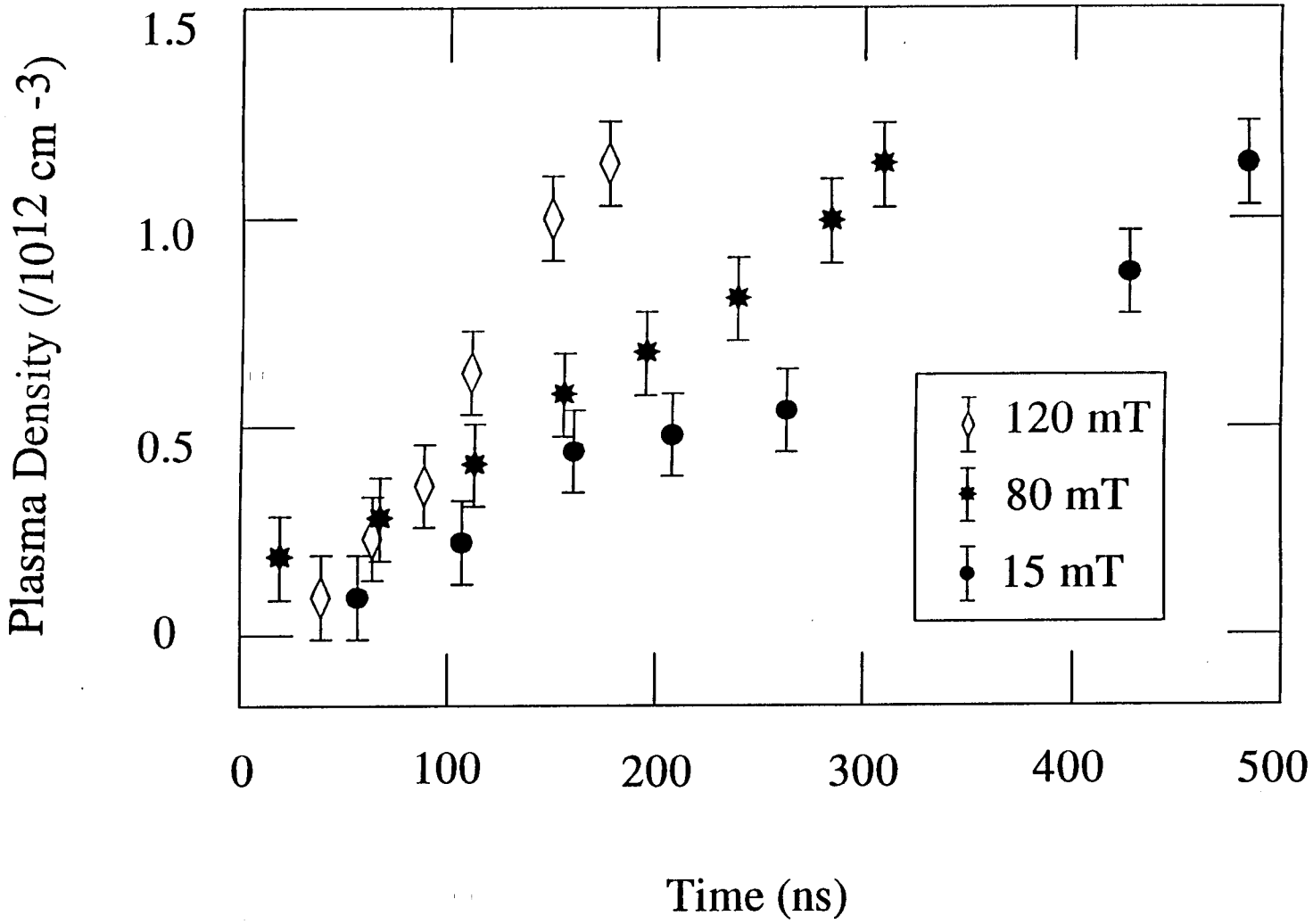
Plasma Density (/1012 cm -3)
1.5
1.0
0.5
0
0
100
200
300
400
500
Time (ns)
120 mT
80 mT
15 mT

Figure 3

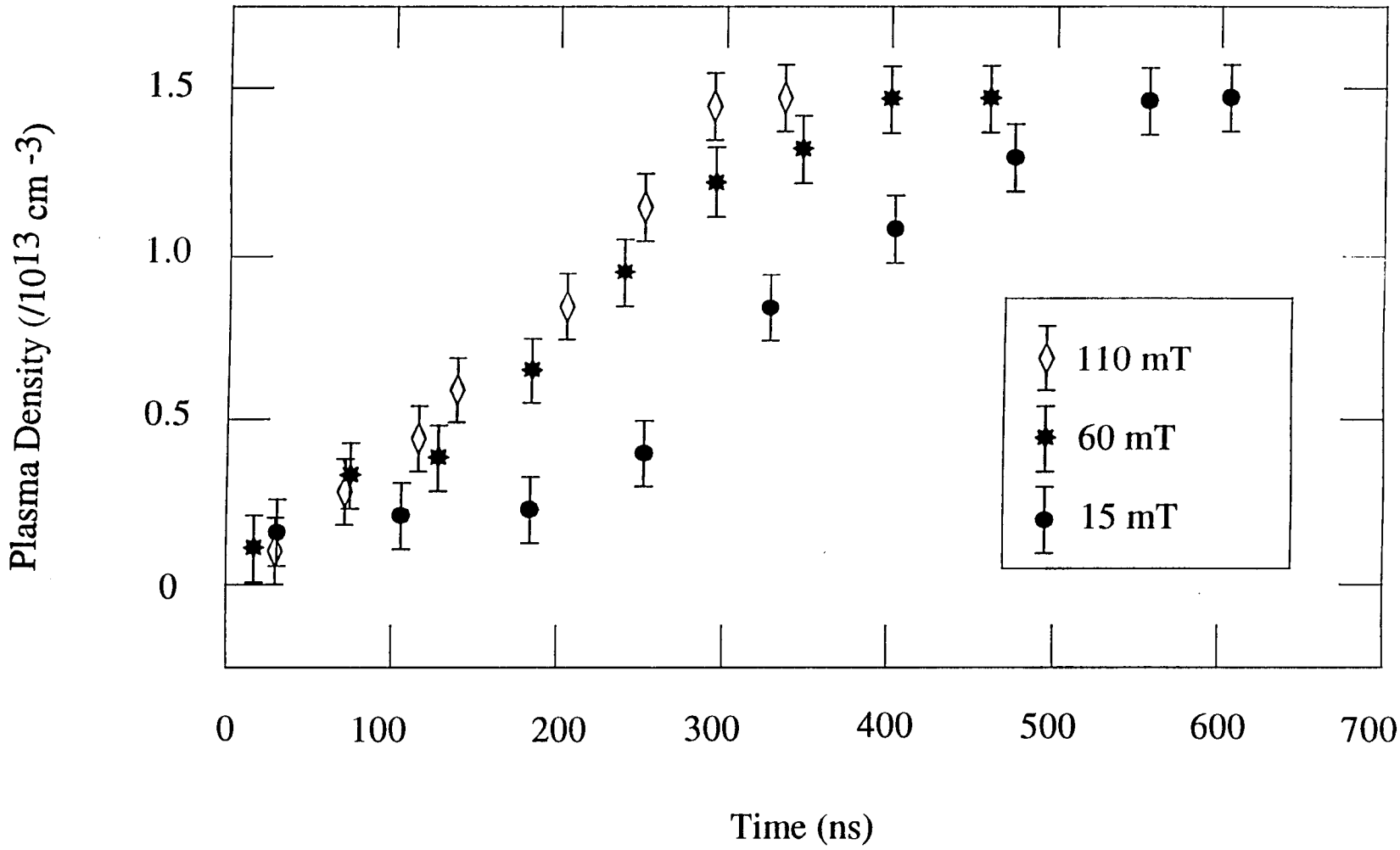
Plasma Density (/1013 cm -3)
1.5
1.0
0.5
0
0
100
200
300
400
500
600
700
Time (ns)
110 mT
60 mT
15 mT

Figure 4

Experimental Study of a Plasma-Filled Backward Wave Oscillator

Xiaoling Zhai, Eusebio Garate, Robert Prohaska, Gregory Benford, and Amnon Fisher, *Member IEEE*

Abstract— **We present experimental studies of a plasma-filled X-band backward wave oscillator (BWO). Depending on the background gas pressure, microwave frequency upshifts of up to 1 GHz appeared along with an enhancement by a factor of 7 in the total microwave power emission. The bandwidth of the microwave emission increased from $\leq$ 0.5 GHz to 2 GHz when the BWO was working at the rf power enhancement pressure region. The rf power enhancement appeared over a much wider pressure range in a high beam current case (10–100 mT for 3 kA) as compared to a lower beam case (80–115 mT for 1.6 kA). The plasma-filled BWO has higher power output compared to the vacuum BWO over a broader region of magnetic guide field strength. Trivelpiece–Gould modes (T–G modes) are observed with frequencies up to the background plasma frequency in a plasma-filled BWO. Mode competition between the Trivelpiece–Gould modes and the X-band TM_{01} mode prevailed when the background plasma density was below 6×10^{11} cm^{-3}. At a critical background plasma density of $n_{cr} \cong 8 \times 10^{11}$ cm^{-3} power enhancement appeared in both X-band and the T–G modes. Power enhancement of the S-band in this mode collaboration region reached up to 8 dB. Electric fields measured by the Stark-effect method were as high as 34 kV/cm while the BWO power level was 80 MW. These electric fields lasted throughout the high power microwave pulse.**

I. Introduction

INTENSE relativistic electron beam excitation of slow wave structures has been an active subject since Nation [1] confirmed the possibility in 1972. Many vacuum slow wave devices have been studied [2]–[6] since, with conversion efficiency of beam kinetic energy into microwaves as high as 30%. Using current pulse power technology, vacuum backward wave oscillators (BWO's) can emit microwave power as high as 1 GW [7]–[8]. Injecting plasma into the slow wave structure [9]–[11] enhances power emission by factors of 3 to 8, however, the basic mechanism is not well understood. All previous plasma-filled BWO experiments concentrated on producing higher power microwaves, higher efficiency and longer pulses. This work studies (a) the effect background plasma has on microwave frequency f and bandwidth Δf; (b) the plasma modes (Trivelpiece–Gould modes) in the plasma-filled BWO and their effect on the BWO waveguide mode (TM_{01}); and (c) measuring the electric field properties in the plasma-filled BWO through the atomic light emission (spectroscopic method).

Manuscript received May 25, 1992; revised September 20, 1992. This work was supported in part by AFOSR under Contract 90-0255.

The authors are with the Physics Department, University of California, Irvine, CA 92717.

IEEE Log Number 9206341.

Filling a slow wave supporting structure with plasma modifies its original dispersion characteristics. The presence of the plasma allows propagation of electromagnetic (EM) waves with frequency below the plasma frequency, f_p, the Trivelpiece–Gould (T–G) modes [12]. A recent calculation [13] analyzed the low frequency modes in a plasma-filled BWO. Of particular interest in this calculation were modes that could axially bunch the electron beam so that stimulated electromagnetic emission could occur. Analyzing electron beam coupling to the modes showed instability for a dense set of frequencies below the plasma frequency, f_p. In addition to the T–G modes of the system, the plasma-filled BWO supports EM waves with $f > f_p$, which can axially bunch the electron beam. These are the usual TM_{0n} modes of the plasma-filled BWO system, modified by addition of the plasma [14]. The TM_{01} mode of the plasma-filled BWO is the mode for which enhanced power output has been previously observed [9]–[11]. It has been suggested that the T–G modes could play an important role [14] in the TM_{01} mode power enhancement. We previously reported [15] detection of T–G modes in a plasma filled BWO, and the correlation between T–G modes and the BWO TM_{01} mode.

Plasma can also affect the BWO rf spectrum. A recent theoretical description of the plasma-filled BWO [16] showed that the addition of plasma results in a frequency upshift in the output of the BWO, the amount of shift depending on the plasma density, n_p. An upshift up to 2.5 GHz was predicted for $n_p = 8 \times 10^{11}$ cm^{-3} for the BWO geometry considered (same as our BWO geometry) with no information about how bandwidth changes with plasma density. Our experimental measurement [12] indicated an upshift of about 1 GHz at $n_p = 8 \times 10^{11}$ cm^{-3}.

Behavior of the electric field in the plasma filled BWO, in a region where the relativistic electron beam, high power rf and plasma interact, could add important information for understanding the basic mechanisms of plasma-filled slow wave devices. To measure the electric field in the center of the BWO, spectroscopic methods can be employed. This method will not interfere with the basic interaction mechanisms, and the high level electromagnetic noise will not affect the measurement. In this paper, we also present results of spectroscopic measurement of the electric field in the plasma filled BWO.

II. Experimental Setups

In our experiment (Fig. 1), a Marx capacitor bank generates a 650 kV, 2 kA voltage pulse with 500 ns pulse duration. The electron beam was produced by field emission from a graphite-

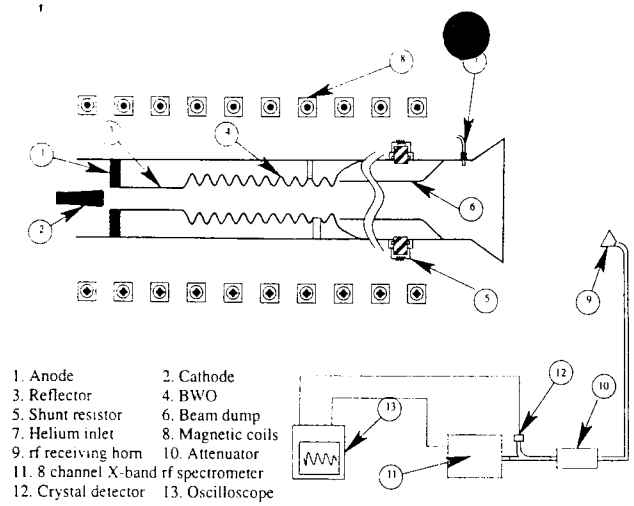

Fig. 1. Experimental setup.

cathode. The beam is annular with 1.8 cm diameter and 2 mm thickness, and is injected into the BWO along a guiding magnetic field. The BWO is a cylindrical waveguide with a periodically varying wall radius, $R(z)$, sinusoidally rippled about the mean radius, R_0, such that

$$R(z) = R_0 + h\cos(k_0 z)$$
$$k_0 = 2\pi/z_0 \tag{1}$$

where $h = 0.45$ cm is the ripple amplitude, $z_0 = 1.67$ cm is the period, and $R_0 = 1.45$ cm. (This BWO copies that of the University of Maryland [10], [14] experiments.) Beam current and voltage were monitored near the cathode, with down stream current measured by a shunt resistor. The BWO was immersed in a 6–18 kG guiding magnetic field. An X-band horn placed 2 m from the end of the drift tube received the microwave emission from the BWO. The microwaves were guided through 20 m of X-band waveguide into a screen room. Here the microwaves were measured by a crystal detector and an X-band 8 channel microwave spectrometer, covering 8.2 GHz $< f <$ 12.4 GHz. Each channel had a bandwidth of approximately 0.5 GHz. The spectrometer filters had 50 dB stopband insertion loss with 0.9 dB passband insertion loss.

Our window for the spectroscopic measurement (Fig. 2) was on the ninth ripple of the BWO (total ten ripples). We used two lenses to image the photons from the BWO center to the optical fibers. The first, with a short focal length, focused light from the center to the second lens. The second lens, with a much longer focal length, focused light to the optical fibers. This setup was chosen to match the f-number of the optical fibers. Two optical fibers transferred the light to a screen room 20 m away from the source. Both fibers were silicon, which has high efficiency and doesn't produce much light when hit by background X-rays. A 1 mm core diameter fiber looked at the allowed line $\lambda = 501.56$ nm from the helium (we used helium plasma). To improve light gathering efficiency for the forbidden lines we used a liner bundle consisting of 50 small fibers with 200 mm diameter. The end near the light source was circular with 1.6 mm diameter, and the other end was a 12 mm long array to match the entrance slit of the monochromator. Both monochromators had a holographic blazed grating with 1800 grooves/mm; the reciprocal linear dispersion of the instrument was 0.7 nm/mm. The detectors were two Hamamatsu R 1894 and R 1635 photomultiplier tubes, both with 0.8 ns rise time. Outputs from the photomultiplier tubes were then recorded by a Tektronix DSA 602 Digitized oscilloscope (1 Gs/s). To prevent systematic error, the spectroscopic system was calibrated daily with a helium discharge lamp. In order to be sure that only the helium emission could be recorded by the photomultiplier, we tuned the two monochromators to the helium allowed and forbidden lines with no helium in the system, and got less than a total of 10 photons over more than 20 shots.

The observation window was also used for the T–G mode measurement. A coaxial cable extended through one window into the BWO with the center conductor acting as a microwave antenna (Fig. 3). Microwaves went through more than 30 m of RG-9 cable, which attenuates the rf signal at 0.7 dB/m for 4 GHz and ~1 dB/m for 9 GHz. Low frequency microwaves were measured with a crystal detector, or with 8 channel S-band (2.6 GHz $< f <$ 3.9 GHz) and J-band (5.85 GHz$< f <$ 8.2 GHz) microwave spectrometers. Each channel of the S-band spectrometer covered approximately 160 MHz bandwidth with the J-band channels covering approximately 294 MHz bandwidth. In both microwave spectrometers the filters had 50 dB stopband insertion loss with 0.9 dB passband insertion loss. We measured frequencies between 3.9 GHz and 5.85 GHz with high pass filters (right circular cylinders with holes drilled along the axis; the hole radius determined the cut-off frequency), since we had no C-band spectrometer. Frequency-resolved measurements below 2.6 GHz were not made due to lack of diagnostic equipment.

Fig. 4 is the experimental setup for the plasma density measurement. We choose helium plasma because of its simple spectrum which also made the spectroscopic measurement easier. Plasma was produced by background helium gas ionization from the electron beam. As shown in Fig. 1, helium gas was injected from one end of the drift chamber and pumped out by the diffusion pump at the other end. Adjusting the helium inlet valve and the pumping speed maintained the helium pressure in the BWO at a constant of a few mT to 150 mT. The injected electron beam produced plasma by beam impact ionization, with $n_p(t)$ adjusted by controlling the gas pressure in the chamber. To measure the plasma density, we used a 10 kW, 4 μs pulse duration, 9.6 GHz X-band magnetron as the rf source. In order to avoid strong X-band TM_{01} radiation and to not modify the oscillator, we replaced our BWO with a stainless steel tube of 10 mm radius, keeping anode and cathode geometry the same. Since the X-band radiation consistently arrived 140 ns ($\pm$10 ns) into the beam pulse, we could correlate the microwave signal with the plasma density measurement at the turn on of the microwaves. However, this measurement most likely underestimates the plasma density during the high power rf emission. The magnetron rf was fed through the plasma by X-band waveguide, carrying information about plasma density $n_p(t)$ in its phase change $\Delta f(t)$. The probe rf was fed through an X-band bandpass filter (8.2 GHz–12.4 GHz) to limit the noise from beam radiation, then it was mixed with rf from

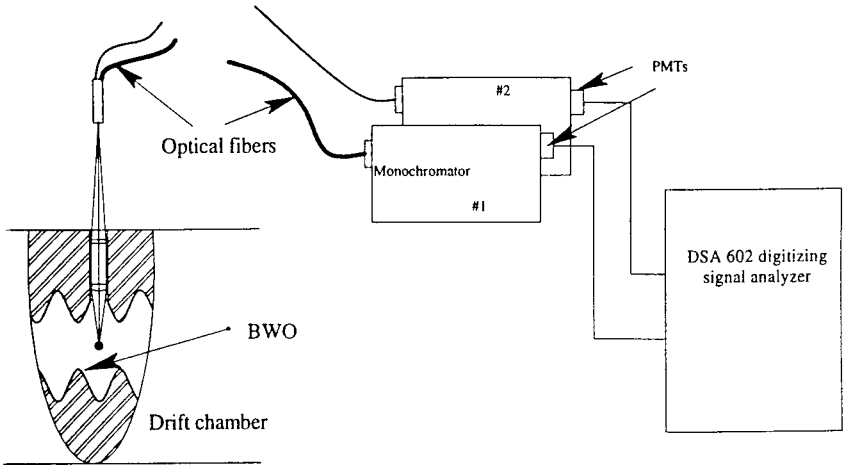

Fig. 2. Spectroscopic system.

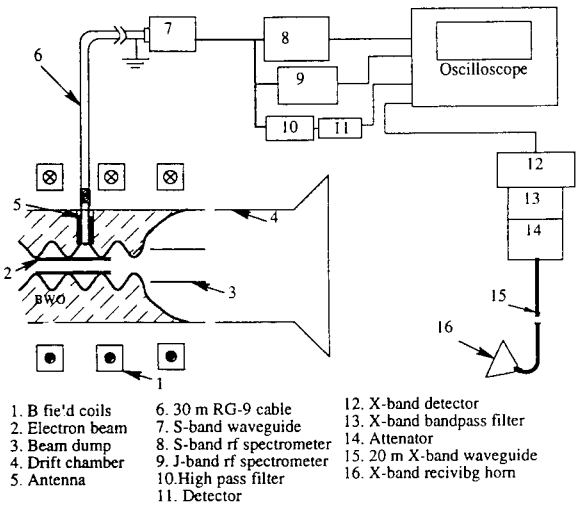

Fig. 3. Experimental setup for Trivelpiece–Gould modes measurement.

a local oscillator so that a mixed frequency of ~100 MHz was obtained. The phase shift $\Delta f(t)$ occurs in the frequency difference $f_M(t) = f_{magnetron} - f_{oscillator}$ as a frequency change $\Delta f_M(t)$. $\Delta f(t)$ can be obtained by comparing this new frequency to the unshifted mixed frequency $f_{M0} = f_M(t < t_0, t_0$ is the beam start time), so that $\Delta f_M(t) = f_M(t) - f_{M0}$. We used this method, rather than a conventional interferometer, where one source is needed, to avoid high levels of broadband X-band noise from the electron beam. The heterodyne technique and the large magnetron input power circumvented this problem by allowing us to use high attenuation in the detector arm. With no plasma in the system, we detected no shift in the frequency difference Δf_{M0}, for up to 3 μs. The beam voltage pulse was synchronized with the stable portion of the mixed frequency. The results of this measurement are presented in Fig. 5.

III. Experimental Results and Discussion

A. Dependency of rf Power and Spectrum on the Plasma Density

This experimental investigation of the plasma-filled BWO started with studying the effect of plasma on the BWO microwave power output level and microwave spectrum. First, we measured the vacuum BWO rf output. Fig. 6(a) shows the beam voltage and the eight channel X-band microwave spectrometer signals from the vacuum BWO for 3 kA beam current. In the vacuum BWO rf signal appeared ~140 ns after the beam turned on, this time delay was independent of the beam current for $I = 3$ kA, 2 kA, and 1.6 kA. Microwave output was always in the first channel of the spectrometer (8.2 to 8.725 GHz, 8.46 GHz center frequency). Maximum power emission was about 80 to 100 MW with microwave pulse duration of 50 ns (FWHM). We calculated the rf power by measuring the power angular distribution, then integrating overall space. Considering our beam pulse was 500 ns, the 50 ns rf pulse was very short. However, when the BWO operated at lower level powers, the microwave emission lasted longer. For example, microwave radiation with power output of 30–40 MW lasted between 130 ns and 150 ns.

As helium was added to the device, we observed a change in the BWO rf power output level and the rf spectrum, but the rf pulse still appeared at ~140 ns into the beam pulse. At low gas pressure (under 10 mT) and $I = 3$ kA only channel 1 and 2 of the spectrometer detected microwaves. However, in the pressure region of rf power enhancement (50 mT $< P_{He} <$ 80 mT), signals appeared in the first four channels of the spectrometer. It is interesting to note that the signal in channel 1 was never less than the vacuum BWO output level, and actually its output was the largest among all channels when the background helium pressure was below 25 mT. When the helium pressure was between 25 mT and 50 mT, rf signals appeared in the first three channels of the spectrometer, and the signal amplitude in the second and third channel increased to the same level as the first channel. At the pressure for maximum power, the third channel detected the largest signal. This indicted a frequency upshift of 1 GHz. Fig. 6(b) shows a shot taken at 60 mT with 3 kA beam current. If we sum the signal output from all channels of the spectrometer in Fig. 6(b) and compare to the signal in Fig. 6(a), it is more than seven times larger. Comparison also shows the bandwidth, Δf, increased from $\leq$0.5 GHz in vacuum to 2 GHz. We observed similar frequency upshift and bandwidth increase for the 1.6 kA case as well. Microwave emission bandwidth as a function

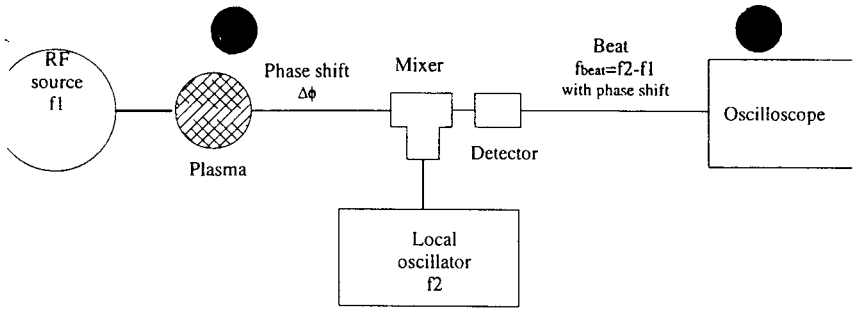

Fig. 4. Experimental setup for the plasma density measurement.

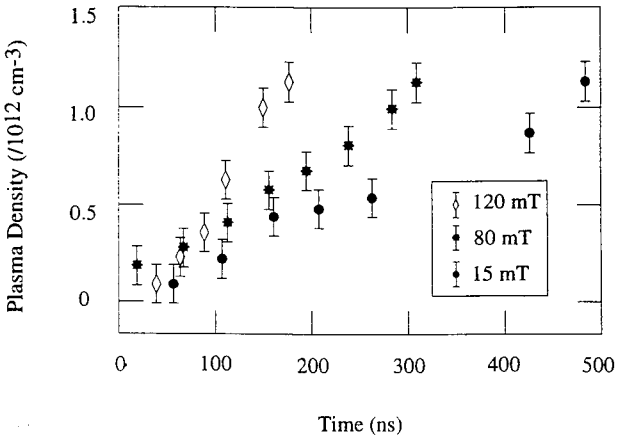

Fig. 5. Plasma density as a function of time for three different helium pressures. Beam start at $t = 0$, and beam current is 1.6 kA. The rf pulse in the BWO arrives at $t \sim 140$ ns. This is likely an underestimate of the plasma density in the BWO since there is no high power rf.

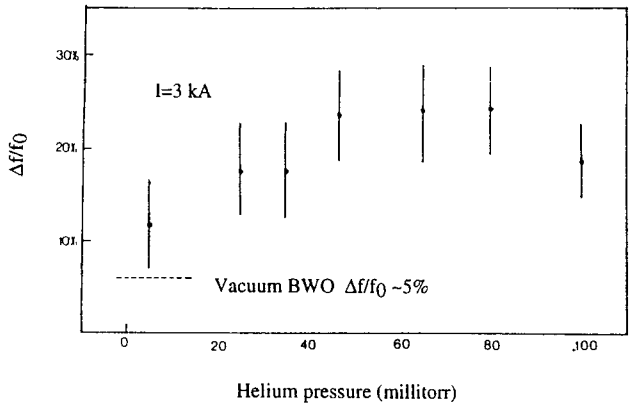

Fig. 7. Bandwidth of the microwave pulses vs. background helium pressure. Δf is the frequency range of microwave output, f_0 is the vacuum rf center frequency. Error is about $\pm 5\%$ due to the sensitivity of our frequency measurement.

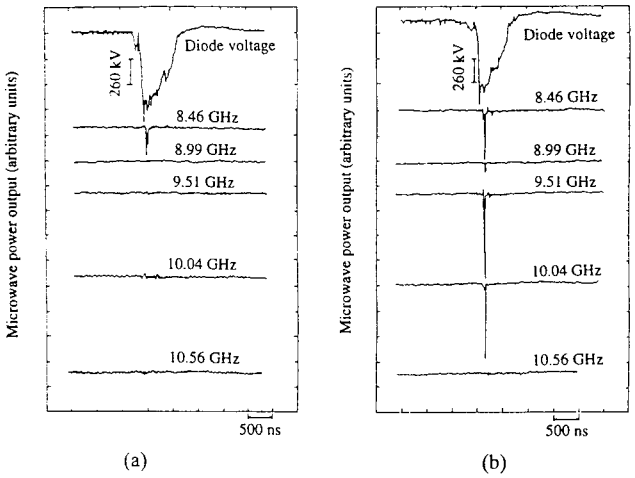

Fig. 6. Oscilloscope traces from the microwave spectrometer and the beam voltage: (a) vacuum BWO, (b) plasma filled BWO (60 mT, $I = 3$ kA). The center frequency of each channel is indicated.

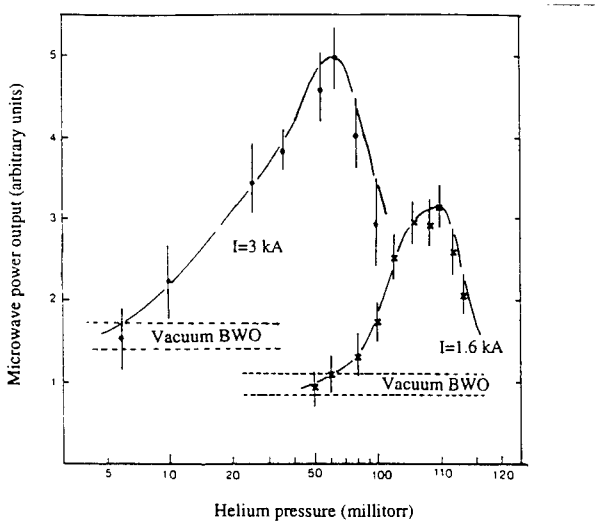

Fig. 8. Microwave power output vs background helium pressure for beam currents of 3 and 1.6 kA. Microwave output for the vacuum BWO is given by the dashed lines. The plasma density as a function of time for the $I = 1.6$ case can be found in Fig. 5.

of the background helium pressure is shown in Fig. 7. The percentage bandwidth $\Delta f/f_0$ changed from $\leq 5\%$ in vacuum to 25% at the pressure of maximum power enhancement. As shown in Fig. 6(b), rf pulse duration is shorter in the higher frequency channels, i.e., the pulse duration in channel 1 is about 30 ns, but is only 10 ns in channel 4.

With 3 kA of beam current injected into the helium-filled BWO, we observed microwave power enhancement for helium pressure between 10 mTorr to 100 mTorr, with maximum power at 60 mT. When the beam current was reduced to 1.6 kA, the power enhancement began at ~80 mT, peaked at 110 mT, then declined. In Fig. 8, the output is the summation of all the signals from channel 1 to channel 4 of the spectrometer ($8.2 \leq f \leq 10.8$ GHz) while the vacuum BWO microwave power output (dashed line) was the signal from the first channel ($8.2 \leq f \leq 8.7$ GHz).

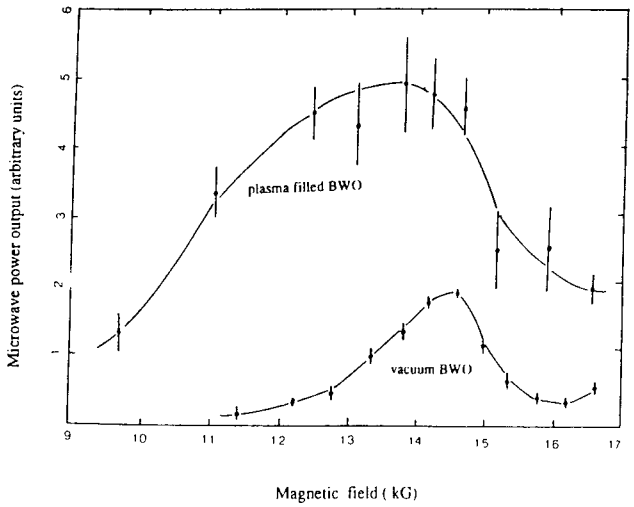

Fig. 9. Microwave power output vs. guiding magnetic field in both vacuum and plasma-filled BWO's.

Microwave power depended on the guiding magnetic field, B, both for vacuum and plasma-filled BWO's (Fig. 9). In the plasma-filled BWO, we kept the background helium pressure in the maximum rf output range, e.g., at ~60 mTorr for the 3 kA beam current. Microwave power peaked around 13.5 kG, with a wider range compared to the vacuum BWO. The vacuum BWO peaked at a slightly larger B field ~14.5 kG. Our 13.5 kG field is much higher than the peak rf emission field (9–10 kG) reported in [2] in their helium-gas-filled BWO. We are not sure of the reason for this difference.

Overall, our BWO generated between 560 ~ 700 MW ($8.2 \leq f \leq 10.8$ GHz) microwave power with plasma, and 80 ~ 100 MW ($8.2 \leq f \leq 8.725$ GHz) in vacuum. rf power enhancement appeared over a much wider pressure range for high beam currents than for the lower current driven BWO. Microwave frequency upshifted 1 GHz in the microwave power enhancement background helium pressure region for both 1.6 kA and 3 kA of beam current. This is less than the theory of [14], which predicts a 2.5 GHz upshift at $n_p = 8 \times 10^{11}$ cm^{-3} (Our plasma density measurements indicate $n_p \geq (8 \pm 1.5) \times 10^{11}$ cm^{-3}.) The background plasma increases the beam electron kinetic energy by reducing the space charge potential produced by the beam in the BWO. This will shift the beam wave intersection point up in frequency. However, a simple calculation based on the interaction of the uncoupled dispersion curve for the BWO and the electron beam yield a frequency upshift of less than 200 MHz for our electron beam parameters. Along with the frequency upshift, bandwidth increased with plasma density. Although the rf pulse duration decreased from 50 ns in vacuum to about 20 ~ 30 ns in plasma filled-BWO, this is not sufficient to account for the observed bandwidth increase.

B. T-G Modes in the Plasma-Filled BWO

Our second step was to look for rf emission (T–G modes) in the plasma-filled BWO, using the antenna placed in the ninth ripple of the BWO, and also using an S-band microwave horn at the end of the chamber. Broadband low frequency microwave radiation was detected up to the plasma frequency of the background plasma. This appeared only with plasma in the BWO, at frequencies below the cutoff frequency of the plasma-filled BWO and lower than the plasma frequency f_p. Power and pulse duration depended on n_p. When the background helium pressure was lower than 70 mT ($n_p < 4 \times 10^{11}$ cm^{-3}, $f_p < 5.7$ GHz), there was no rf signal in the J-band spectrometer. rf appeared in every channel of the S-band spectrometer with about the same amplitude and pulse duration. The T–G mode emission ($f < 5.7$) GHz correlated with the X-band TM_{01} mode emission. As in Fig. 10, T–G mode power emission always dropped when the TM_{01} mode peaked. This mode competition appeared every shot for about 100 shots when $n_p < 4 \times 10^{11}$ cm^{-3}. As plasma density rose to 4×10^{11} cm^{-3} the TM_{01} mode power output showed no change. However, the T–G mode emission power gradually increased by a factor of 2 over a plasma density change of 2 to 4×10^{11} cm^{-3} (4 GHz$< f_p < 5.7$ GHz). As the pressure reached 100 mT ($n_p \sim 7 \times 10^{11}$ cm^{-3}, $f_p = 7.5$ GHz), rf signals appeared in the first seven channels of the J-band spectrometer (eighth channel overlapped with the X-band TM_{01} emission) and every channel of the S-band spectrometer. The S and J-band spectrometer signals lasted ~100 ns. Signals in J-band had smaller amplitude than that of the S-band. However, since we could not determine the coupling efficiency of the antenna as a function of frequency, and the presence of the S-band waveguide (Fig. 3), we cannot determine quantitative differences in S and J-band signals.

As the background helium pressure reached 120 mT ($n_p = n_{cr} \sim 8 \times 10^{11}$ cm^{-3}, $f_p \sim 8$ GHz) a simultaneous peak in the TM_{01} mode and the T–G modes (both S and J-band) was observed (Fig. 10(c)). A sudden enhancement appeared in the S-band T–G mode peak power of up to 8 dB. The J-band rf signal amplitude increased with the S-band rf but no more than 3 dB. The X-band TM_{01} mode emission increased for 6×10^{11} cm^{-3} $< n_p < 8 \times 10^{11}$ cm^{-3} and peaked at n_{cr}. Power enhancement was typically a factor of 3 at n_{cr}, but up to a factor of 6 in some shots. This enhancement in X-band TM_{01} mode radiation for plasma filled BWOs has been observed by others [9], [10]. Possible mechanism of the enhancement can be found in [18] and [19]. The correlation and enhancement of the T–G modes in a plasma filled BWO was discussed in [14].

Given the error in the plasma density measurement, the background plasma density could be as high as $n_p \sim 9.5 \times 10^{11}$ cm^{-3} ($f_p \sim 8.8$ GHz) when the TM_{01} mode and T–G modes power emission are enhanced. This could indicate the possibility that part of the enhanced X-band signal came from T–G mode radiation. Although the absolute T–G modes power emission was not calibrated, when a 27dB (constant attenuation for $0 < f < 18$ GHz) attenuator was placed in series with the detector and the RG-9 cable, the X-band rf could still be detected in the eighth bin of the J-band spectrometer (7.9 GHz$< f <$ 8.2 GHz) but not the lower frequencies of the band. This indicated that the power carried by the T–G modes emission (in J-band) was at least 27 dB less than the X-band TM_{01} mode. For plasma density $n_p > 8 \times 10^{11}$ cm^{-3}, power emission in the TM_{01} mode gradually decreased, and the T–G modes pulse became much

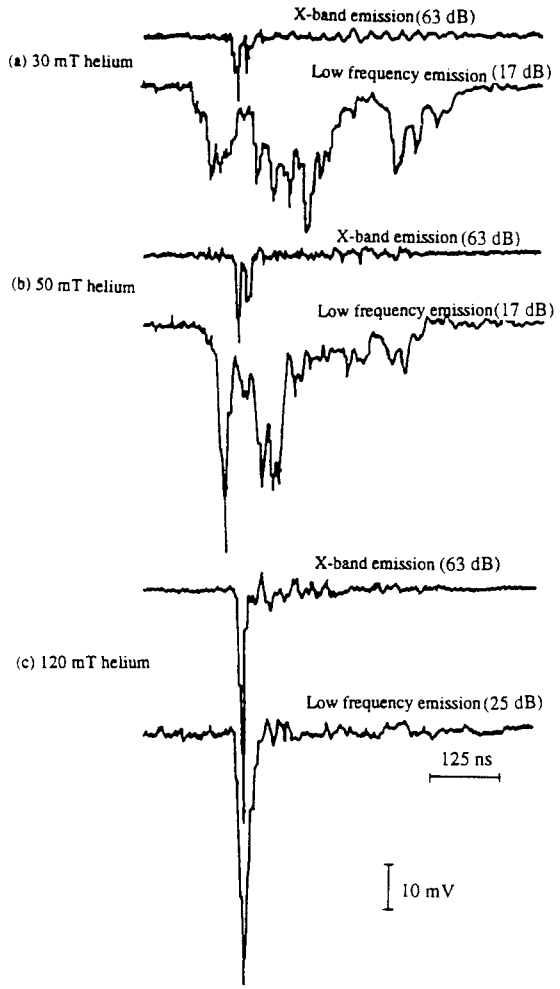

Fig. 10. Oscilloscope traces of the X-band (8.2–10.2 GHz, measured by X-band crystal detector) and the Trivelpiece–Gould modes (measured by a crystal detector) microwave signals. The low frequency emission was 2 GHz$< f <$ 5.7 GHz, higher frequencies were cut off by an additional piece of RG-8 cable which attenuated rf at 0.7 dB/m at 4 GHz but 6 dB/m at 9 GHz. Frequencies less than 2 GHz were cut off by the S-band waveguide. The attenuation was kept the same for all cases except in the low frequency rf emission in (c), where an additional 8 dB was added. The background helium pressures were (a) 30 mT, (b) 50 mT, (c) 120 mT.

shorter ($\sim$50 ns) but their amplitude kept increasing (both S and J-band). When the pressure reached 170 mT the J and S-band power emission were 2–3 times larger than that of the 120 mT case. We were not able to measure the plasma density for background helium pressure higher than 130 mT, where $n_p \geq 10^{12}$ cm^{-3}, which was beyond the cutoff density for the 9.6 GHz magnetron rf.

To check that this low frequency emission was a result of the plasma present in the BWO, we tested without helium gas ("vacuum", 5×10^{-5} torr). We found broadband low frequency radiation with frequency 2.6 GHz$< f <$ 5.85 GHz appeared very late (200 ns after the TM_{01} rf signal turn off) in the beam pulse, when the beam voltage dropped to less than 200 kV. Nothing was detected in the J-band spectrometer. This puzzle was solved when we sought traces of Cu (wall material) and hydrogen atoms (water absorption on the BWO wall) with our optical spectroscopic system (Fig. 2). Measurements showed very strong hydrogen light from the BWO when the

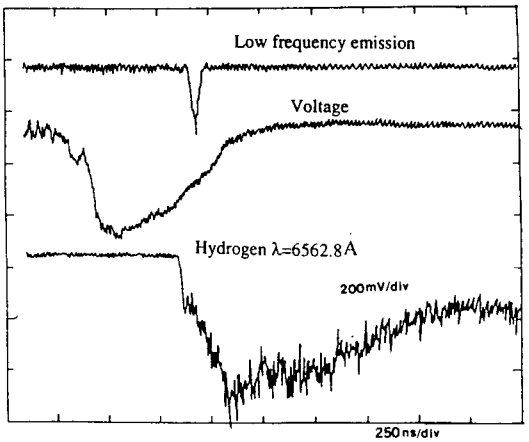

Fig. 11. Upper trace is the low frequency emission from the BWO without the background helium gas. Bottom trace is the light emission from wall plasma.

low frequency radiation appeared (Fig. 11). Simultaneous Cu atomic emission was 20 times weaker than hydrogen radiation. We believe a hydrogen plasma forms from beam impact with adsorbed water, released by beam electrons hitting the BWO wall. The plasma density measurement showed this plasma density reached more than 10^{12} cm^{-3}, but came 200 ns later than the X-band radiation in the system. We also looked for T–G mode emission when we replaced the BWO with the tube of radius 10 mm. Broadband (2.6 GHz$< f <$ 3.9 GHz, measured with the spectrometer and cut off filters) low frequencies emission was observed with amplitude ten times less than that of the plasma-filled BWO case. Also, emission in the smoothbore didn't appear until much later in the beam pulse, e.g., for 30 mT helium, low frequencies appeared 300 ns into the beam pulse, but in the plasma-filled BWO low frequencies started with the beam. Using the theory of [20], a calculation using cylindrical tube geometry indicates T–G modes with $v_{\text{phase}} = v_{\text{beam}}$ don't exist until $n_p \sim 2.9 \times 10^{12}$ cm^{-3} ($v_{\text{beam}} = 0.8c$ for $V = 400$ kV when T–G modes emission appeared). A gradient in plasma density of $\sim 3\%$ can account for the frequency spectrum. Our plasma density measurement showed that at 30 mT, n_p reached 10^{12} cm^{-3} about 300 ns after the beam started (see Fig. 5), consistent with the observed time of low frequency emission. At higher background gas pressure, the low frequency signals appeared much earlier in the beam pulse, because at higher pressure plasma density reached 2.9×10^{12} cm^{-3} much earlier.

In this part of the measurement, we measured broadband, low frequency microwaves in our plasma-filled BWO with a spectrum of 2.6 GHz$< f <$ 7.85 GHz, without attempting to observe $f <$ 2.6 GHz. We believe these waves arise from electron beam excitation of the "dense" spectrum of T–G modes discussed in [13], because at low helium pressure the low frequency emission from the plasma-filled BWO appeared as soon as the beam turned on, which we didn't see in the plasma-filled smoothbore case with the same gas pressure and beam current. Only in a plasma-filled BWO can one expect to see T–G modes with $v_{\text{phase}} = v_{\text{beam}}$ ($v_{\text{beam}} = 0.9c$ for $V = 650$ kV) when the plasma density is low. We also saw power increases of up to a factor of 2 in the broadband, low

frequency radiation ($f < 5.7$ GHz) when n_p rose from 2 to 4×10^{11} cm^{-3}. At $n_{cr} \sim 8 \times 10^{11}$ cm^{-3} a simultaneous and sudden enhancement in both the T–G ($f < 7.85$ GHz) and X-band output were observed. We are not sure why the low frequency in S-band of the T–G modes showed more power enhancement (up to 8 dB) at n_{cr} than that of the higher frequencies in J-band (only 3 dB). The exact mode structure of the T–G modes and the absolute power was not calibrated because of our limited diagnostic tools.

C. Electric Field Measurement

Using spectroscopic methods to measure electric field distributions in a relatively high noise level system is efficient and convenient. This method has been used in many laboratories [21]–[25] since Baranger and Mozer suggested in 1961 using the high-frequency Stark effect as a diagnostic tool to study the frequency and strength of the electrostatic fluctuations in a plasma [25]. We choose the four energy-level system (3^1P, 3^1D, 2^1P, 2^1S) of helium I for spectroscopic measurement. Transitions from 3^1P to 2^1S ($\lambda_A = 501.56$ nm) and from 3^1D to 2^1P ($\lambda = 667.80$ nm) are allowed, and the transition from 3^1P to 2^1P is forbidden ($\lambda_F = 663.20$ nm) in the electric dipole approximation. In a perturbing electric field, energy levels 3^1D and 2^1P are mixed; therefore, it is possible to see photons from the forbidden line. The perturbing electric field strength can be calculated [23] by the forbidden ($\lambda_F = 663.20$ nm) and allowed ($\lambda_A = 501.56$ nm) line intensity ratio (I_F/I_A):

$$E = 305.8\left(\frac{I_F}{I_A}\right)^{0.54} \text{ kV/cm.} \quad (2)$$

In these studies we increased the diode A–K gap reducing the beam current to ~1 kA, to get a longer microwave pulse. Forbidden line photons appear with the high power microwave emission, while allowed line photons appear earlier and last much longer than the rf pulse (Fig. 12). This is because the forbidden transition only happens when there are electric fields in the system, while the allowed transition occurs as long as there is plasma, exciting the helium electrons to higher energy levels. This suggests that the electric fields inducing the forbidden transitions were produced by the high power rf. We counted photon numbers in each time interval for both the forbidden and allowed lines in each shot, then averaged over ~100 shots. The ratio of the average photon numbers in the forbidden and allowed lines was used to calculate the electric field with (2).

Fig. 13 shows the results of the electric field measurement in the plasma-filled BWO when the rf was enhanced by the background plasma by a factor of 2 over its vacuum counterpart. The measured rf power was 80 MW±10 MW and the rf pulse duration (FWHM) was ~60 ns. Fig. 13 shows the electric fields lasted only as long as the microwave pulse, peaking at 34 kV/cm, then dropping to ~12 kV/cm.

When the background plasma density was ~10^{12} cm^{-3}, the X-band rf turned off. At the same time an rf signal appeared in Ku-band with center frequency of 14.6 GHz and ~150 ns pulse duration. This is the mode switching from the TM_{01}

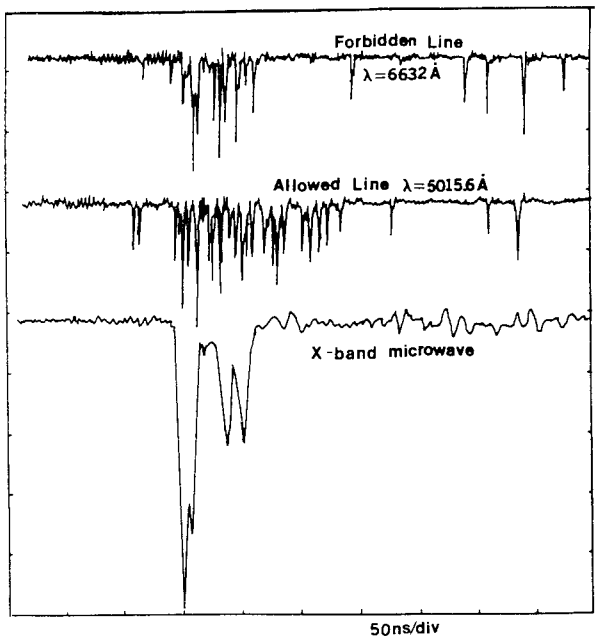

Fig. 12. Oscilloscope trace of the forbidden and allowed line photons and the microwave pulse.

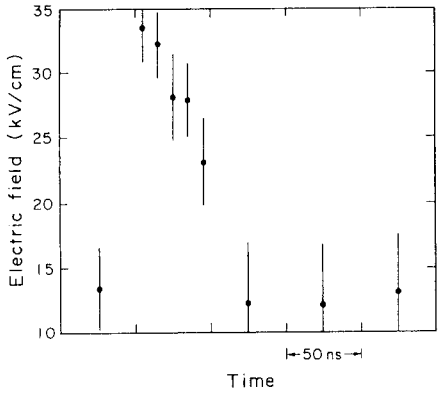

Fig. 13. Electric field vs. time when the BWO rf power was enhanced by the background plasma.

mode to the TM_{02} mode in the plasma-filled BWO, as reported and discussed in [14]. Electric fields present in the plasma filled BWO were measured when the mode switching occurred. The measured electric field strength after mode switching was about 16 kV/cm (Fig. 14) and lasted 150 ns, as long as the TM_{02} microwave pulse.

To estimate how much microwave power this field strength implies, assume a smooth wall tube with radius of $R_0 = 1.9$ cm (this measurement was done in the wide part of the BWO where $r = 1.9$ cm). Assuming a TM_{0n} mode propagating along the axis, we have

$$S = \frac{c}{8\pi}\frac{1}{\sqrt{\mu\epsilon}}\left(\frac{\omega}{\omega_{\lambda n}}\right)^2\sqrt{\left(1-\frac{\omega_{\lambda n}^2}{\omega^2}\right)} \cdot E_0^2\int_0^{R0}\left[J_0\left(\frac{\gamma_{0n}r}{R_0}\right)\right]^2 2\pi r dr. \quad (3)$$

Here S is the power flux of the rf in the tube, with $\omega/2\pi = 9.5$ GHz, the center rf frequency of the plasma-

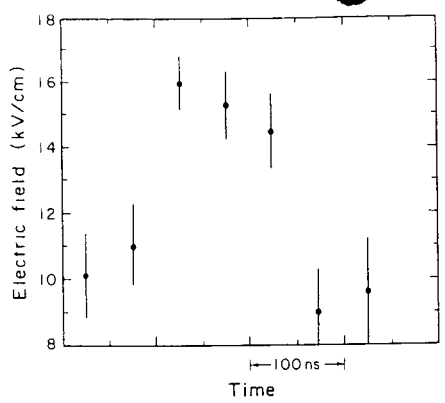

Fig. 14. Electric field vs. time when mode switching occurred.

filled BWO, γ_{0n} is the nth root of $J_0(r)$, and $\omega_{\lambda n}$ is the cut-off frequency of the tube for the TM_{0n} mode, and E_0 is the amplitude of the electric field. The quantity we measured is $\overline{E} = \sqrt{\langle E^2 \rangle} = 34$ kV/cm. To get E_0^2 we have:

$$E_0 = 1.41\sqrt{\langle E^2 \rangle}. \tag{4}$$

For the TM_{01} mode, (3) and (4) give $S = 19 \pm 11$ MW, with the uncertainty due to the 30% error in electric field measurement. Direct microwave power measurement gives 80 MW$\pm$10 MW.

This 34 kV/cm electric field is lower than we expected from the direct rf power measurement, since it gives a power flux lower than the measured X-band microwave power and there were other waves (Trivelpiece–Gould modes) in the plasma-filled BWO which contribute to $\overline{E}$. Although the Trivelpiece–Gould mode had 20 dB less power than the X-band TM_{01}, it could produce electric fields $\sim$1 kV/cm. Using the same method as for the TM_{01} mode, we estimated that the TM_{02} mode rf power emission was only 0.3 MW. Some error may come from the assumption of a TM_{0n} mode propagating axially in a 19 mm radius smooth tube with a average electric field the same as our measured field value. The actual measurement was done in a rippled wall BWO. In a BWO, the electric field distribution of a TM_{0n} mode peaks near the BWO wall rather than on the axis. To accurately calculate the power flux in the BWO, one has to know the electric field distribution $\vec{E}(\vec{r})$ in the BWO and the light collecting efficiency as a function of position in the BWO, a very complex calculation. We have not done this calculation at this time. The electric field from the electron beam charge is not important here. For the 1 kA beam the beam density is $\sim 5 \times 10^{11}$ cm^{-3} whereas n_p was as high as 8×10^{11} cm^{-3} when the rf pulse appeared and the electric field peaked. Therefore, the beam was charge neutralized.

IV. Conclusion

In conclusion, we have observed microwave frequency upshifts of up to 1 GHz and a bandwidth increase from ≤ 0.5 GHz to 2 GHz along with an enhancement by a factor of 7 in the total microwave power emission in our plasma filled BWO. We also measured T–G modes with frequencies up to the background plasma frequency in our plasma-filled BWO. This could be the "dense spectrum" of plasma waves as discussed in [13]. At a critical plasma density the T–G modes and the BWO TM_{01} mode output power were simultaneously enhanced. The T–G mode measurement and the electric field measurement, to the best of our knowledge, have not been done previously for a device of this kind. In the plasma filled BWO, we measured the average electric field strength as a function of time on our BWO axis, where the relativistic electron beam, high power microwaves and plasma interact. While the microwave power output was enhanced by the background plasma, the electric field peaked at 34 kV/cm and lasted only as long as the high power rf pulse, about 50 ns.

Acknowledgment

We thank Dr. K. Kato, David Sar and General Dynamics, Pomona Division, for the use of their equipment.

References

[1] J. A. Nation, "On the coupling of an high-current relativistic electron beam to a slow wave structure," *Appl. Phys. Lett.*, vol. 17, no. 11, pp. 491–494, Dec. 1970.

[2] Y. Carmel, J. Ivers, R. E. Kribel, and J. Nation, "Intense coherent Cherenkov radiation due to the interaction of a relativistic electron beam with a slow-wave structure," *Phys. Rev. Lett.*, vol. 33, no. 12, pp. 1278–1282, July 1974.

[3] M. Friedman, "Emission of intense microwave radiation from an auto-modulated relativistic electron beam," *Appl. Phys. Lett.*, vol. 26, no. 7, pp. 366–368, April 1975.

[4] V. I. Belousov, V. V. Bunkin, A. V. Gaponov-Grekhov *et al.*, "Intense microwave emission from periodic relativistic electron bunches," *Sov. Tech. Phys. Lett.*, vol. 4, no. 12, pp. 584–585, Dec. 1978.

[5] V. S. Ivanov, N. F. Kovalev, S. I. Krementsov, and M. D. Raizer, "Relativistic millimeter carcintron," *Sov. Tech. Phys. Lett.*, vol. 4, pp. 329–330, July 1978.

[6] N. I. Zaitsev, N. F. Kovalev, G. S. Korablev, I. S. Kulagin, and M. M. Ofitserov, "Relativistic carcinotron with $\lambda = 3$ cm and pulse length of 0.4 μs," *Sov. Tech. Lett.*, vol. 7, no. 7, pp. 477–378, July 1981.

[7] Yu. F. Bondar', S. I. Zavorotnyi, A. L. Ipatov, N. I. Karbushev, N. F. Kovalev, O. T. Loza, G. P. Mkheidze, and L. E' Tsopp, "Measurement of rf emission from a carcinotron with a relativistic electron beam," *Sov. J. Plasma Phys.*, vol. 9, no. 2, pp. 223–226, March–April 1983.

[8] V. S. Ivanov, S. I. Krementsov, V. A. Kutsenko, M. D. Raizer, A. A. Rukhadze, and A. V. Fedotov, "Investigation of a relativistic Cerenkov self-generator," *Sov. Phys. Tech. Phys.*, vol. 26, no. 5, pp. 580–583, May 1980.

[9] Yu. V. Tkach, Ya. B. Fainberg, I. I. Magda, N. I. Gaponenko, G. V. Skachek, S. S. Pushharev, N. P. Gadetskii, and A. A. Belukha, "Microwave emission in the interaction of a high-current relativistic beam with a plasma-filled slow-wave structure," *Sov. J. Plasma Phys.*, vol. 1, no. 1, pp. 43–46, Jan.–Feb. 1975.

[10] Y. Carmel, K. Minami, R. A. Kehs, W. W. Destler, V. L. Granatstein, D. Abe, and W. L. Lou, "Demonstration of efficiency enhancement in a high-power backward-wave oscillator by plasma injection," *Phys. Rev. Lett.*, vol. 62, no. 20, pp. 2389–2492, May 1989.

[11] X. Zhai, E. Garate, R. Prohaska and G. Benford, "Study of an X-band backward wave oscillator," *Appl. Phys. Lett.*, vol. 60, no. 19, pp. 2332–2334, May 1992.

[12] A. W. Trivelpiece *et al.*, "Space charge wave in cylindrical plasma columns," *J. Appl. Phys.*, vol. 30, no. 11, pp. 1784–1793, Nov. 1959.

[13] W. R. Lou, Y. Carmel, W. W. Destler, and V. L. Granatstein, "New mode in a plasma with periodic boundaries: the origin of the dense spectrum," *Phys. Rev. Lett.*, vol. 67, no. 18, pp. 2481–2484, Oct. 1991.

[14] Y. Carmel, K. Minami, W. R. Lou, R. A. Kehs, W. W. Destler, V. L. Granatetein, D. K. Abe, and J. Rodgers, "High-power microwave generation by excitation of a plasma-filled rippled boundary resonator," *IEEE Trans. Plasma Sci.*, vol. 18, pp. 497–506, June 1990.

[15] X. Zhai, E. Garate, R. Prohaska, and G. Benford, "Observation of Trivelpiece–Gould modes in a plasma-filled backward wave oscillator," *Phys. Rev. A*, vol. 45, no. 12, pp. 8336–8339, June 1992.

[16] K. Minami, Y. Carmel, V. L. Granatstein, W. W. Destler, W. R. Lou, D. K. Abe, R. A. Kehs, M. M. Ali, T. Hosokawa, K, Ogura, and

T. Watanabe, "Linear theory of electromagnetic wave generation in a plasma-loaded corrugated-wall resonator," *Plasma Sci.*, vol. 18, pp. 537–544, June 1990.

[17] K. Minami, W. R. Lou, W. W. Destler, R. A. Kehs, V. L. Granatsein, and Y. Carmel, "Observation of a resonant enhancement of microwave radiation from a gas-filled backward wave oscillator," *Appl. Phys. Lett.*, vol. 53, no. 7, pp. 559–561, May 1988.

[18] A. T. Lin and L. Chen, "Plasma-induced efficiency enhanced in a backward-wave oscillator," *Phys. Rev. Lett.*, vol. 63, no. 26, pp. 2808–2811, Dec. 1989.

[19] M. Botton and Amiran Ron, "Efficiency enhancement of a plasma filled backward-wave oscillator by self-induced distribution feedback," *Phys. Rev. Lett.*, vol. 66, no. 19, pp. 2468–2471, May 1991.

[20] E. P. Garate, A. Fisher, and W. Main, "High-gain plasma Cerenkov maser," *IEEE J. Quantum Electronics*, vol. 25, no. 7, pp. 1712–1719, Jul. 1989.

[21] A. Dovrat and G. Benford, "Optical diagnosis of electric fields in a beam-driven turbulent plasma," *Phys. Fluids B*, vol. 1, no. 12, pp. 2488–2491, Dec. 1989.

[22] H. -J. Kunze and H. R. Griem, A. W. DeSilva, G. C. Goldenbaun, and I. J. Spalding, "Spectroscopic investigation of enhanced plasma oscillation in a high-voltage theta pinch," *Phys. Fluids*, vol. 12, no. 12, pp. 2669–2676, Dec. 1969.

[23] K. Kawasaki, T. Usui, and T. Oda, "Forbidden transition in helium and lithium due to fluctuating electric field for plasma diagnostics," *J. Phys. Soc. Jpn*, vol. 51, pp. 3666–3671, May 1982.

[24] G. C. A. M. Janssen, E. H. A. Granneman, and H. J. Hopman, "Observation of high-frequency fields due to the interaction of a relativistic electron beam with a plasma," *Phys. Fluids*, vol. 27, no. 3, pp. 736–745, March 1984.

[25] M. Baranger and B. Mozer, "Light as a plasma probe," *Phys. Rev.*, vol. 123, no. 1, pp. 25–28, Feb. 1961.

Xiaoling Zhai, photograph and biography not available at the time of publication.

Eusebio Garate, photograph and biography not available at the time of publication.

Robert Prohaska, photograph and biography not available at the time of publication.

Gregory Benford, photograph and biography not available at the time of publication.

Amnon Fisher (M'86) photograph and biography not available at the time of publication.